

## Estimates on the Possible Annual Seismicity of Venus

Iris van Zelst<sup>1,2</sup> , Julia S. Maia<sup>1,3</sup> , Ana-Catalina Plesa<sup>1</sup> , Richard Ghail<sup>4</sup> , and Moritz Spühler<sup>1</sup> 

### Key Points:

- An inactive Venus with global background seismicity like Earth's continental intraplate seismicity has a few hundred quakes  $\geq M_w 4$  per year
- A lower bound on an active Venus where fold belts, coronae, and rifts are seismically active predicts a few thousand quakes  $\geq M_w 4$  annually
- The upper bound for an active Venus results in thousands (~5,000–18,000) venusquakes  $\geq M_w 4$  per year

### Supporting Information:

Supporting Information may be found in the online version of this article.

### Correspondence to:

I. van Zelst,  
iris.vanzelst@dlr.de;  
iris.v.zelst@gmail.com

### Citation:

van Zelst, I., Maia, J. S., Plesa, A.-C., Ghail, R., & Spühler, M. (2024). Estimates on the possible annual seismicity of Venus. *Journal of Geophysical Research: Planets*, 129, e2023JE008048. <https://doi.org/10.1029/2023JE008048>

Received 9 AUG 2023  
Accepted 10 JUL 2024

### Author Contributions:

**Conceptualization:** Iris van Zelst  
**Data curation:** Iris van Zelst, Julia S. Maia, Richard Ghail, Moritz Spühler  
**Formal analysis:** Iris van Zelst, Julia S. Maia  
**Funding acquisition:** Iris van Zelst, Ana-Catalina Plesa  
**Methodology:** Iris van Zelst, Richard Ghail  
**Supervision:** Iris van Zelst  
**Visualization:** Iris van Zelst, Julia S. Maia  
**Writing – original draft:** Iris van Zelst  
**Writing – review & editing:** Iris van Zelst, Julia S. Maia, Ana-Catalina Plesa, Richard Ghail, Moritz Spühler

© 2024. The Author(s).

This is an open access article under the terms of the [Creative Commons Attribution License](https://creativecommons.org/licenses/by/4.0/), which permits use, distribution and reproduction in any medium, provided the original work is properly cited.

<sup>1</sup>Institute of Planetary Research, German Aerospace Center (DLR), Berlin, Germany, <sup>2</sup>Centre of Astronomy and Astrophysics, Technical University of Berlin, Berlin, Germany, <sup>3</sup>Université Côte d'Azur, Observatoire de la Côte d'Azur, CNRS, Laboratoire Lagrange, Nice, France, <sup>4</sup>Department of Earth Sciences, Royal Holloway, University of London, Egham, UK

**Abstract** There is a growing consensus that Venus is seismically active, although its level of seismicity could be very different from that of Earth due to the lack of plate tectonics. Here, we estimate upper and lower bounds on the expected annual seismicity of Venus by scaling the seismicity of the Earth. We consider different scaling factors for different tectonic settings and account for the lower seismogenic thickness of Venus. We find that 95–296 venusquakes equal to or bigger than moment magnitude ( $M_w$ ) 4 per year are expected for an inactive Venus, where the global seismicity rate is assumed to be similar to that of continental intraplate seismicity on Earth. For the active Venus scenarios, we assume that the coronae, fold belts, and rifts of Venus are currently seismically active. This results in 1,161–3,609 venusquakes  $\geq M_w 4$  annually as a realistic lower bound and 5,715–17,773 venusquakes  $\geq M_w 4$  per year as a maximum upper bound for an active Venus.

**Plain Language Summary** Venus could be seismically active at the moment, but it is uncertain how many earthquakes (or to use the proper term: venusquakes) there could be in a year. Here, we calculate the minimum and maximum number of venusquakes we could expect in a given year on Venus based on different assumptions. If we assume there is not much seismic activity on Venus (comparable to the interior of tectonic plates on Earth), we find that we could expect about a few hundred venusquakes per year with a magnitude bigger than or equal to 4. For an estimate of the maximum amount of venusquakes, we assume that Venus has regions with more seismic activity: the so-called coronae, fold belts, and rifts. Depending on our assumptions, we then find that more than 17,000 venusquakes with a magnitude bigger than or equal to 4 could occur in a year.

## 1. Introduction

After the successful mapping of the Venusian surface by Magellan from 1990 to 1992, for a long time the prevailing hypotheses for Venus' geodynamic regime were that of a catastrophic or episodic resurfacing regime. The reason for this was the observation of a relatively low number of craters with a near-random spatial distribution on the surface (932 craters; Strom et al., 1994), from which people deduced a uniform, relatively young surface age of 240–800 Myr (Le Feuvre & Wiczorek, 2011; McKinnon et al., 1997). In these catastrophic or episodic resurfacing scenarios, Venus is currently in a relatively quiet tectonic phase after the geologically recent resurfacing event that led to the observed young surface age (O'Rourke et al., 2023; Rolf et al., 2022). However, the impact crater observations are also consistent with models in which volcanic and tectonic activity occurs at roughly constant rates over time (e.g., Herrick et al., 2023).

Indeed, in recent years the view on Venus' current tectonic activity has shifted toward a more active planet, rivaled in the Solar System only, perhaps, by our own Earth. From a geodynamical point of view, other theories for its geodynamic regime have been put forward, such as the plutonic squishy lid regime (Lourenço et al., 2020), which are consistent with ongoing activity on Venus today. Additionally, the shift toward an active Venus is partly induced by compelling evidence from Magellan, Pioneer Venus, and Venus Express data that Venus might be currently volcanically active. Data from Venus Express shows regions of high thermal emissivity which could be associated with chemically unweathered rocks (Smrekar et al., 2010). The thermal emissivity anomalies correlate with volcanic rises, such as Imdr Regio (Smrekar et al., 2010), indicating geologically recent volcanism in these regions. Depending on the assumption of tectonic regime and amount of volcanic flux, Smrekar et al. (2010) estimate that the bright spots represent recently active volcanoes younger than ~2.5 Myr, and potentially as young as 250,000 years or less. Similarly, weathering experiments at Venusian temperature and pressure conditions

suggest that the reduction of surface thermal emissivity occurs on time scales of  $\sim 500,000$  years (Dyar et al., 2021). Other weathering experiments at Venusian temperatures (but Earth pressures; see Gilmore et al., 2023, for an overview) have even suggested that this weathering is a rapid process on the order of tens to hundreds of years (Zhong et al., 2023) or even months to years (Filiberto et al., 2020). Additionally, low radar emissivity values, which indicate there is a low amount of high dielectric minerals formed by weathering, typically spatially correspond to the observed thermal emissivity anomalies. Brossier et al. (2022) therefore postulate that these observed low radar emissivity values in Ganis chasma could be the result of volcanic eruptions in the last 30 years, indicating that Venus is volcanically active now (Filiberto et al., 2020). The variability in  $SO_2$  concentration in the clouds observed by Pioneer Venus and Venus Express from 1979 to 2011 has also been attributed to recent volcanic eruptions (Marcq et al., 2013). The most compelling evidence for active volcanism on Venus to date comes from Herrick and Hensley (2023) and Sulcanese et al. (2024), who observed changes in three different volcanic regions by analyzing consecutive radar images acquired by Magellan. They interpreted these changes as new volcanic flows and hence ongoing volcanic activity on Venus. In addition, recent gravity and topography analysis indicate that Venus has a thin low viscosity zone which could be interpreted as an indication of partial melting in the mantle (Maia et al., 2023). In line with that, recent estimates from scaling the volcanism of Earth to Venus yield 12–42 volcanic eruptions on Venus in a year, depending on assumptions on the amount of volcanism associated with plume-induced subduction at coronae (Byrne & Krishnamoorthy, 2022; Van Zelst, 2022). Future missions such as VERITAS (Smrekar et al., 2020) and EnVision (Ghail et al., 2016) will provide better constraints on Venus' volcanic activity (Widemann et al., 2023, and references therein).

In the meantime, since Venus seems to be geologically active, it is reasonable to assume that it is also seismically active. Indeed, its seismicity could be more extensive than that of Mars and the Moon, which are both believed to be significantly less tectonically active than Venus (Stevenson et al., 2015). On these bodies, despite being in a stagnant lid regime, seismicity has been observed with the successfully deployed Apollo Lunar Surface Experiments Package on the Moon (Nakamura et al., 1982) and on Mars with the InSight mission (Banerdt et al., 2020). As Venus is now thought to be in a more tectonically active geodynamic regime than a stagnant lid (Rolf et al., 2022), its potential seismicity is thought to be at least comparable with Earth's intraplate seismicity (Ganesh et al., 2023; Stevenson et al., 2015; Tian et al., 2023). On top of that, observed rift systems (Ivanov & Head, 2011), fold belts (Byrne et al., 2021), wrinkle ridges (Sabbeth et al., 2023a), and coronae (Davaille et al., 2017; Gülcher et al., 2020) could still be actively deforming at present and hence be potentially seismically active. There are even speculations that the Venera 14 lander recorded microseisms from far-away seismicity in the active Beta Regio on Venus, although there are many other potential explanations for these recorded signals (Ksanfomaliti et al., 1982).

Besides a large variety of tectonic features with potential Earth analogs, the crust of Venus has properties similar to the Earth's crust. Considering their similarities is important when assessing if seismicity might be governed by the same processes and therefore manifest in the same manner in the two planets. Direct compositional measurements from the Soviet landers have shown that the surface of Venus has a similar composition to that of mid-oceanic ridge basalts on Earth (e.g., Abdrakhimov & Basilevsky, 2002). Moreover, the average crustal thickness of Venus has been estimated to be approximately 15–20 km (James et al., 2013; Maia & Wiczorek, 2022), which is comparable to the thickness of Earth's oceanic crust. Considering these similarities, it is reasonable to use Earth's seismic activity as a starting point to better understand the level of seismicity expected for Venus.

Here, we estimate upper and lower bounds of the amount of seismicity that could be expected for an active Venus, as well as an inactive Venus with seismicity reminiscent of intraplate seismicity on Earth. By scaling the seismicity of the Earth to Venus in Section 2 for different tectonic settings, that is, using the same philosophy as Byrne and Krishnamoorthy (2022) that Earth analogs can be applied to Venus, we obtain our results (Section 3). We then discuss our assumptions and the likely differences between the seismicity on Earth and Venus caused by, for example, their different lithospheric temperature structures, water content, and hence overall lithospheric strength structure, in Section 4. In this section, we also discuss and compare with seismicity estimates of previous studies and comment on how the actual seismicity of Venus could be determined in the future. This is followed by our conclusions in Section 5.

## 2. Methods

In order to estimate the seismicity of Venus, we use a global earthquake catalog for Earth and sort the earthquakes into different tectonic areas on the globe, thereby obtaining an effective “seismicity density” for each tectonic

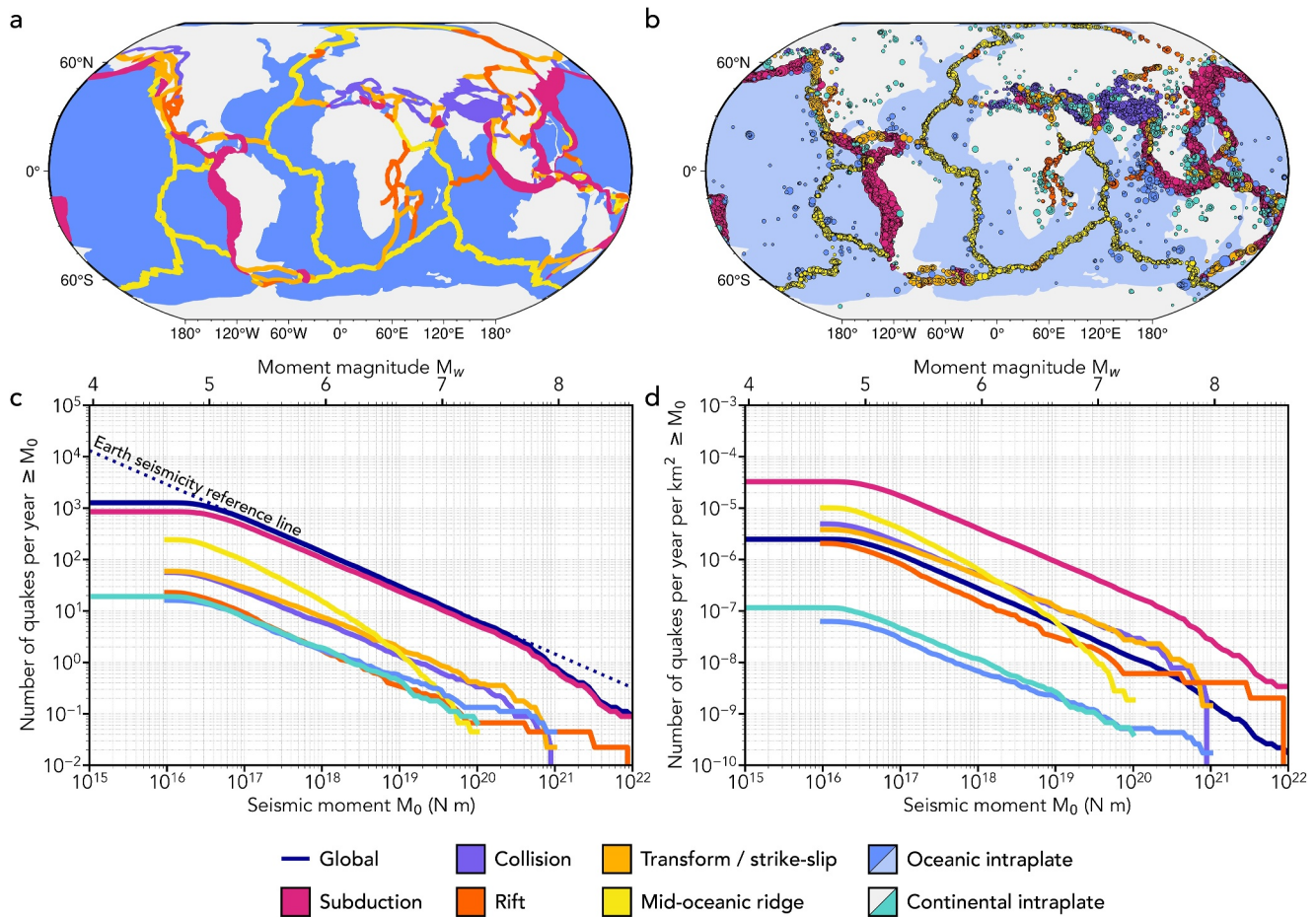


**Figure 1.** (a) Map of the Earth showing how its surface area is divided into seven discrete tectonic settings. (b) Earthquakes in the Centroid Moment Tensor (CMT) catalog from 1976 to 2020 colored according to tectonic setting with the symbol size proportional to the earthquake magnitude. (c) Annual earthquake size-frequency distribution for the Earth based on the CMT catalog and split into different tectonic settings. The dotted dark blue line is a reference line for Earth's seismicity extrapolated from the size-frequency distribution for seismic moments of  $10^{17}$  to  $10^{19}$  N m to lower and higher seismic moment assuming a constant slope ( $b$ -value). Note that this means that the Earth's reference line overestimates the amount of quakes with moment magnitudes larger than 8. (d) Seismicity density on the Earth for different tectonic settings, that is, number of earthquakes in the CMT catalog per year per  $\text{km}^2$ . Maps are in Robinson projection.

setting. This “seismicity density” is defined as the number of quakes per year per  $\text{km}^2$  for each tectonic setting. Hence, it is effectively the averaged regional  $b$ -value per  $\text{km}^2$ . We then apply this same seismicity density to analogous Venusian settings to obtain three different possible estimates of Venus' current seismicity: an estimate for an inactive Venus and an upper and lower bound for an active Venus, depending on the assumptions that we make. In this section, we present our methods in detail.

## 2.1. Tectonic Settings on Earth

To obtain the seismicity density of different tectonic settings on Earth, we calculate the area of seven different tectonic settings on the Earth. For this, we use the recent maps of global geological provinces and tectonic plates from Hasterok et al. (2022). We define subduction and collision zone areas according to the zones of deformation defined by Hasterok et al. (2022), as the location of the seismicity associated with these types of plate boundaries typically encompasses a large, diffuse area. We extend the deformation zones of Hasterok et al. (2022) to account for deep earthquakes associated with subduction zones that lie outside of the deformation zones defined at the surface of the Earth. We further define the areas of transform and strike-slip regions, rift zones, and mid-oceanic ridges according to the mapping of Hasterok et al. (2022) by defining a 150 km wide band on either side of the respective plate boundary and correcting for overlapping areas. The remaining surface area of the Earth is divided into oceanic intraplate and continental intraplate regions, according to the mapped oceanic and continental crust

by Hasterok et al. (2022). Hence, the surface area of the Earth is divided into seven distinct (non-overlapping) tectonic settings: subduction zones (5.13% of Earth's surface area), collision zones (2.23%), transform and strike-slip regions (3.03%), rift zones (2.17%), mid-oceanic ridges (4.70%), and oceanic (50.44%) and continental intraplate (32.30%) regions (Figure 1a, Table S1 in Supporting Information S1).

## 2.2. Seismicity of the Earth

We use the global Centroid Moment Tensor (CMT; Dziewonski et al., 1981; Ekström et al., 2012) earthquake catalog from 1976 to 2020 with a completeness magnitude of  $M_w 5$  to characterize Earth's annual seismicity. There are various methods to convert seismic moment  $M_0$  (in N m) into moment magnitude  $M_w$  (e.g., Beroza & Kanamori, 2015; Stein & Wysession, 2009). Throughout our study, we follow Beroza and Kanamori (2015) by using the following expression:

$$\log M_0 = 1.5M_w + 9.05. \quad (1)$$

We sort the earthquakes of the CMT catalog in the predefined tectonic areas (Figure 1b) and obtain an earthquake size-frequency distribution for the different tectonic settings (Figure 1c). The seismicity density for each of the tectonic settings found on Earth is then calculated by dividing the earthquake size-frequency distribution by the surface area (Figure 1d; Table S1 in Supporting Information S1).

Subduction zones have the highest seismicity density, followed by the other plate boundary settings and the overall global seismicity density of the Earth (Figure 1d). The seismicity density of collision zones and strike-slip regions are similar, with a slightly lower seismicity density for the rift zones. Intraplate seismicity clearly has the lowest seismicity density (approximately one order of magnitude less than the global seismicity density) with the continental intraplate seismicity density being slightly higher than the oceanic intraplate seismicity density.

## 2.3. Tectonic Settings on Venus

For Venus, we consider three different tectonic settings in this study: Venusian rifts (chasmata), fold belts characterized by compressional deformation, and the volcano-tectonic corona features, for which we show representative examples in Figure 2 and their distribution on the surface of Venus in Figure 3a. For each of these tectonic settings, we assign plausible, potential Earth analogs to obtain an estimate of the potential annual seismicity of Venus. We refrain from explicitly including other tectonic settings found on Venus, such as tesserae and wrinkle ridges, because they do not have clear Earth analogs, which makes their seismicity density unconstrained in our methodology. On bodies that are generally considered to be in the stagnant lid geodynamical regime, like Mars (e.g., Golombek et al., 1992; Knapmeyer et al., 2006) and the Moon (e.g., Williams et al., 2019), wrinkle ridges have been successfully used to estimate the background seismicity. Wrinkle ridge seismicity has also been considered for Venus, with Sabbeth et al. (2023a) estimating the potential seismicity of wrinkle ridges based on mapped fault lengths, which we discuss in detail in Section 4. Here, we instead consider the area of Venus outside the mapped rifts, fold belts, and coronae as an intraplate tectonic setting (Figure 3a), thereby implicitly assigning intraplate-like seismicity densities to tectonic settings like wrinkle ridges and tesserae.

### 2.3.1. Rift Zones

Rifts on Venus are typically defined as large, broad structural units of 100 km or more that are characterized by closely spaced extensional structures (Ivanov & Head, 2011; Price & Suppe, 1995). They are similar to the so-called groove belts on Venus, which are smaller and typically contain less dense faulting patterns (Ivanov & Head, 2011). The extensional features in rift zones are often interpreted as normal faulting and horst-and-graben structures, which are typically associated with continental rifting on Earth (Foster & Nimmo, 1996). Indeed, many studies have pointed out both the morphological similarity and the similar amount of crustal extension between rifts on Venus and continental rifts on Earth (e.g., McGill et al., 1981; Phillips et al., 1981; Stoddard & Jurdy, 2012).

For example, Foster and Nimmo (1996) provide a detailed comparison between the Eastern African Rift system on Earth and the rift systems of Beta Regio on Venus. They identified many similarities, including maximum fault segment lengths, and concluded that differences stem from the lack of sediment and larger fault strength on

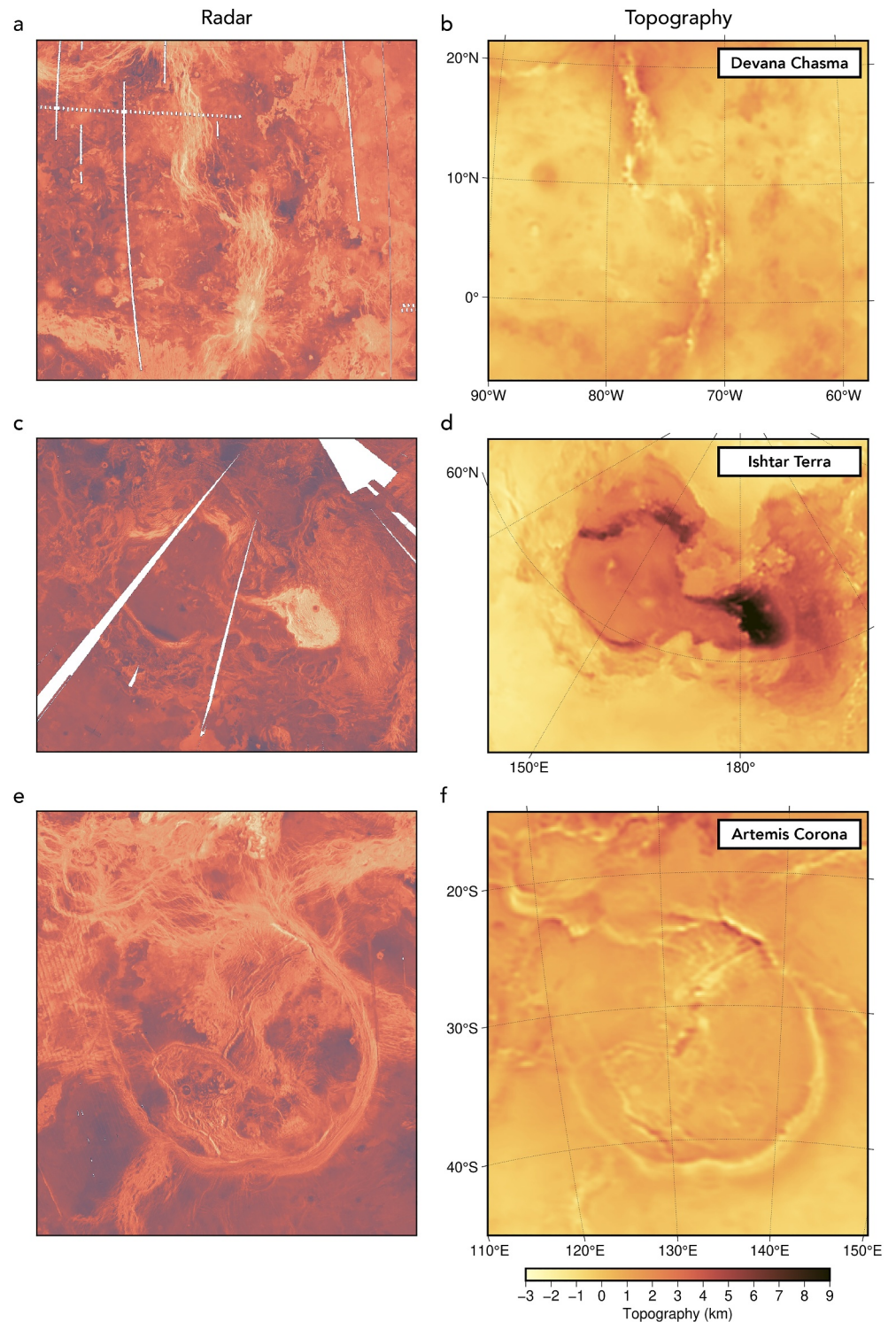


**Figure 2.** Examples of tectonic features on Venus with Magellan radar image mosaics on the left and topography maps derived from the Magellan altimetry data on the right. (a, b) Devana Chasma as an example of a rift system on Venus; (c, d) Ishtar Terra with Maxwell Montes as an example of a region characterized by compressional deformation and classified as a fold belt in this study following Price et al. (1996); (e, f) Artemis Corona, the largest corona on Venus. Maps are in Lambert azimuthal equal-area projection.

Venus. As another example, Graff et al. (2018) suggested that the rift morphologies of Venus could be analogous to the Atlantic Rift System prior to ocean opening.

Modeling studies also indicate that continental rifting is a plausible mechanism to generate the rifting morphologies observed on Venus (Regorda et al., 2023). It is clear, however, that the difference in surface conditions between Venus and Earth plays a role in the rift mechanism as well (Regorda et al., 2023).

The physical mechanisms governing the formation of rifts on Venus are still largely unclear. In general, Venustian rifts are commonly associated with regions suggested to be surface expressions of active mantle plumes, such as Atla, Beta, and Phoebe Regiones (Kiefer & Peterson, 2003; Stofan et al., 1995). As such, continental rifting on Earth could be a reasonable analog for rifts on Venus. However, considering Venus' basaltic crustal composition—potentially more similar to Earth's oceanic crust than its continental crust (Head, 1990)—and increased surface temperature, the rifts on Venus might also bear resemblance to the mid-oceanic ridges on Earth. Indeed, the three largest rift systems on Venus, Parga Chasma, Hecate Chasma, and Dali-Diana Chasma, are not typically associated with hotspots, so the mid-oceanic ridges on Earth might be the best analogy for these settings on Venus.

### 2.3.2. Fold Belts

There are several different types of compressional structures on the surface of Venus, including ridges, ridge belts (defined as closely clustered ridges; Frank & Head, 1990), and mountain belts (Price & Suppe, 1995). Here, we specifically focus on fold belts, defined by Price et al. (1996) as concentrated zones of compressive deformation forming linear ridge belts analogous to terrestrial fold-and-thrust belts. As such, the mapping of fold belts by Price et al. (1996) also includes distinctly compressive regions, such as the mountain belt of Ishtar Terra. The various compressive features on Venus typically resemble each other, but differ in terms of topography (Ivanov & Head, 2011). The origin of these compressional features has been debated, with early studies proposing early stage mantle downwellings as a mechanism (Zuber, 1990). More recently, Byrne et al. (2021) suggested that compressional zones like fold belts bound the globally fragmented crustal blocks in the Venus lowlands and could potentially facilitate movements of the blocks with respect to each other. The timing of the motion of these crustal blocks is hard to constrain (Byrne et al., 2021). Potentially these crustal blocks are still moving to this day, which could imply that the fold belts are still actively deforming at present. Here, we consider continental collision as the most appropriate analog for fold belts on Venus (Jull & Arkani-Hamed, 1995; Phillips & Malin, 1984; Romeo & Turcotte, 2008).

### 2.3.3. Coronae and Corona-Like Features

Coronae are roughly circular structures characterized by an annulus of high deformation (Basilevsky & Head, 1997; Grindrod & Hooenboom, 2006; Ivanov & Head, 2011; Solomon et al., 1991). Their typical topographic rims typically overlap with their fracture annuli (Sabbeth et al., 2024), which could still be seismically active today (Schools & Smrekar, 2024).

Coronae are unique to Venus and their formation is typically associated with volcanism and mantle upwellings (Smrekar & Stofan, 1997; Stofan et al., 1992). There are various topographic signatures associated with coronae, which have been linked to differences in formation mechanisms and stages of formation (e.g., Gülcher et al., 2020; Smrekar & Stofan, 1997). This variety in topographic signatures of coronae has inspired a variety of proposed formation mechanisms for coronae including mantle plumes (Schools & Smrekar, 2024; Smrekar & Stofan, 1999), hot spots (Stofan et al., 1991), and small-scale upwellings (Herrick, 1999; Johnson & Richards, 2003; Koch & Manga, 1996; Musser & Squyres, 1997; Squyres et al., 1992) followed by gravitational relaxation of isostatically uncompensated plateaus (Janes et al., 1992) and associated delamination (Smrekar & Stofan, 1997); magmatic loading of the crust due to transient mantle plumes (Dombard et al., 2007); gravitational Rayleigh-Taylor lithosphere instabilities (Hooenboom & Houseman, 2006); and lithospheric dripping as a result of the interaction between a mantle plume and a rift (Piskorz et al., 2014).

The formation of large coronae, such as Artemis corona, is typically associated with plume-lithosphere interactions where a rising plume impinges on the Venustian lithosphere and causes subduction-like dynamics and delamination at its edges (Baes et al., 2021; Davaille et al., 2017; Gerya, 2014; Gülcher et al., 2020, 2023; Schubert & Sandwell, 1995; Smrekar et al., 2018). For example, Gülcher et al. (2020) used 3-D numerical models to show that different corona structures could represent different plume styles and stages of formation with some

coronae exhibiting subduction-like lithosphere dripping at their edges. Using these modeling insights and comparing to topographic data of Venus, Gülcher et al. (2020) found that 37 of 133 studied coronae (i.e., 27.8%) could be actively forming tectonic structures at present. The remaining coronae that they studied were either deemed to be inactive (26.3%) or inconclusive (45.9%) according to the modeled topography profiles. It is worth noting that the coronae studied in Gülcher et al. (2020) are not the complete set of observed coronae on Venus and are instead biased toward the larger corona structures with a diameter  $\geq 300$  km. Still, their modeling study provides compelling evidence that tectonic processes—and specifically subduction-like processes—could still be active today in a subset of the coronae.

In this study, we mainly follow Gülcher et al. (2020) in assuming that coronae are formed by subduction-like processes associated with plume-lithosphere interactions. Since this is likely only the case for a subset of coronae (e.g., Davaille et al., 2017), we also implicitly consider delamination or plume processes for corona formation (see Section 2.4.2 for more details).

### 2.3.4. The Surface Areas of Different Tectonic Features on Venus

We calculate the surface area covered by rifts (8.25% of Venus' surface area; Jurdy & Stoddard, 2007), coronae (7.76%), and fold belts (i.e., compressional regions; 1.64%) from maps by Price and Suppe (1995) and Price et al. (1996) as shown in Figure 3a (also see Table S2 in Supporting Information S1). We manually ensure that there are no overlapping regions by including rift-associated coronae as part of the rift system. The remaining surface area of Venus that is not assigned an actively deforming tectonic setting is then considered to be intraplate (82.35% of Venus' surface; Figure 3a).

## 2.4. Scaling From the Earth to Venus

To scale from the Earth to Venus, we consider several aspects. First, we assign the seismicity density of analogous tectonic settings on Earth (Sections 2.1 and 2.2) to the tectonic settings we consider for Venus (Section 2.3). Since this is a seismicity density (i.e., the number of quakes per year per  $\text{km}^2$  or the  $b$ -value per  $\text{km}^2$ ), we hereby implicitly scale by surface area, taking into account the differences in surface area that tectonic settings occupy on the two planets and the different global surface area between the two planets as a whole. In addition, we scale with the global estimated average seismogenic thickness to account for the fact that Venus most likely has a lower seismogenic thickness than the Earth, because of its higher surface temperature (see Sections 2.4.1 and 4.1). Hence, since we consider both the different surface areas and seismogenic thicknesses of the two planets, we actually scale by seismogenic volume when going from Earth analogs to Venus settings. Here, we discuss how we scale the seismogenic thickness of the two planets in detail (Section 2.4.1) and we discuss the Earth analog assumptions for our three end-member estimates (Section 2.4.2), as well as the possible extent of our seismicity estimates in terms of minimum and maximum quake magnitudes (Section 2.4.3).

### 2.4.1. Seismogenic Thickness

The seismogenic thickness of a planet's lithosphere is the maximum depth at which earthquakes can nucleate, typically dictated by the temperature structure of the lithosphere and the location of the brittle-ductile transition. Taken over the entire surface area of the planet, the seismogenic thickness transforms into the seismogenic volume.

On Earth, the down-dip limit of the seismogenic zone in subduction zones is estimated to range from 250 to 550°C isotherms depending on the mineralogy (He et al., 2007; Peacock & Hyndman, 1999; Scholz, 2019; Tichelaar & Ruff, 1993). In a slightly narrower estimate, the down-dip limit of the seismogenic zone is typically associated with the 350 and 450°C isotherms for megathrust seismicity (Gutscher & Peacock, 2003; Hyndman & Wang, 1993; Hyndman et al., 1997). In order to explain observations of intermediate-depth and deep seismicity in subduction zones and the existence of double seismic zones in subducted slabs, the 600 and 800°C isotherms are also often cited as the factor limiting seismogenic thickness (Boettcher et al., 2007; Jung et al., 2004; Kelemen & Hirth, 2007; McKenzie et al., 2005; Peacock, 2001; Wang et al., 2017; Yamasaki & Seno, 2003). In high strain rate environments in tectonically active regions, earthquakes have been proposed to occur at temperatures up to 800°C (Chen & Molnar, 1983; Molnar, 2020). There have also been observations of earthquakes in continental lithosphere at depths modeled to correspond with isotherms of 750°C (Prieto et al., 2017) and earthquakes in slabs in regions estimated to exceed 1,000°C (Melgar et al., 2018). In hotspot settings, such as Iceland, the average

temperature at the base of the seismogenic zone has been estimated to be 750°C with a standard deviation of 100°C (Ágústsson & Flóvenz, 2005). Hence, estimates of the temperature defining the maximum seismogenic zone on Earth vary wildly and depend on the tectonic setting. Depending on the thermal structure of the lithosphere, the estimated seismogenic thickness therefore also carries a large uncertainty. In theoretical and modeling studies, the 600°C isotherm is often assumed to be the end-member temperature for brittle failure, and hence seismogenesis, in Earth's lithosphere for simplicity (Emmerson & McKenzie, 2007; Van Zelst et al., 2023).

As a measure of the amount of seismicity, the seismogenic thickness is of limited use as it merely defines the region where quakes could nucleate and slip. Indeed, earthquakes can propagate below the seismogenic depth (e.g., Aderhold & Abercrombie, 2016), although they typically nucleate above it, and there are—depending on tectonic setting—vast regions with a significant seismogenic thickness that experience limited seismicity, for example, the interiors of continental plates, which typically undergo limited deformation. However, despite its limitations, seismogenic thickness is still a useful variable to look at when determining the maximum amount of seismicity that could occur on a given planet.

Since Venus has a higher surface temperature than Earth, assuming the same seismogenic thickness for both planets is likely incorrect. More specifically, we expect Venus to have a lower seismogenic thickness than Earth due to its higher surface temperature and hence shallower brittle-ductile transition in its lithosphere. We therefore need to take the likely difference in seismogenic thickness between the two planets into account when estimating the seismicity of Venus.

In order to estimate the seismogenic thickness scaling factor between Earth and Venus, we first estimate the average seismogenic thickness for the Earth, which is relatively well constrained. For oceanic crust, we assume a representative seismogenic thickness of 36.5 km, which is the depth of the 600°C isotherm (McKenzie et al., 2005; Richards et al., 2018) for the average age of 64.2 Myrs of the oceanic crust (Seton et al., 2020). For an estimate of the average seismogenic thickness of continental crust, we follow Wright et al. (2013), who used coseismic and interseismic observations to arrive at estimates of  $14 \pm 5$  km and  $14 \pm 7$  km of the average continental seismogenic thickness. Regional differences in seismogenic thickness are attributed to compositional differences, differing strain rates, or grain sizes, as Wright et al. (2013) found that there is no clear global relationship between seismogenic thickness and temperature structure for continental crust. So, following Wright et al. (2013)'s study, we assume an average seismogenic thickness of 14 km for continental crust in our calculations. Then, applying the ratio of oceanic to continental crust from Hasterok et al. (2022), we obtain an average seismogenic zone thickness for the Earth of 26.93 km. We note that this is a lower end-member estimate of the average seismogenic zone thickness of the Earth, especially since other studies (e.g., Molnar, 2020) have found that the seismogenic thickness of continental crust is higher than the 14 km suggested by Wright et al. (2013). However, for our purpose of obtaining global end-member seismicity estimates with a reasonable uncertainty margin, this value is adequate to obtain scaling ratios between Earth and Venus as described below.

For Venus, we calculate a likely minimum and maximum seismogenic thickness (see Van Zelst et al., 2024, for the data and scripts used in this study) from proposed end-member thermal gradients of Venus' lithosphere (Bjonnes et al., 2021; Smrekar et al., 2023). Like for our Earth estimate, we calculate the depth corresponding to the 600°C isotherm, as this seems to limit the seismogenic zone on Earth most robustly. Seeing as Venus most likely has a drier interior than the Earth that is absent of volatiles, crustal rocks are stronger compared to their terrestrial counterparts (Mackwell et al., 1998). Hence, brittle deformation could also occur up to deeper isotherms in Venus' interior. Therefore, we also provide seismogenic thickness estimates assuming a temperature of 800°C as the limiting factor in Van Zelst et al. (2024). However, here, we compute end-members of the possible annual seismicity on Venus using the 600°C isotherm, as this provides a better comparison with Earth studies that use the same isotherm value to define the base of the seismogenic layer. To obtain a minimum estimate of Venus' seismogenic zone thickness, we calculate the average thermal gradient for Venusian rifts estimated by Smrekar et al. (2023), which results in a seismogenic thickness of 7.3 km assuming a limiting temperature of 600°C. As a maximum estimate, we use the proposed minimum thermal gradient of 6 K/km for the Mead crater on Venus by Bjonnes et al. (2021), which results in a seismogenic thickness of 22.7 km for a temperature of 600°C at the base of the seismogenic zone. We note that these estimates represent the thermal gradients during the formation of the associated features, but given the young ages predicted for Venus' surface these values are likely representative for its current thermal state.



Combining these estimates of the Venusian seismogenic thickness with that of Earth, we obtain minimum and maximum scaling ratios of 0.27 and 0.84, respectively, to account for the likely difference in seismogenic thickness between Venus and Earth. We note that these end-member scaling ratios are a necessary simplification for our global assessment of the potential seismicity on Venus. Future studies could take a more realistic, regional approach, where the seismogenic thickness varies spatially and for different tectonic settings like on Earth.

### 2.4.2. Three End-Member Estimates

We consider three different scenarios when scaling the seismicity from the Earth to Venus (Table S3 in Supporting Information S1). First, we consider an inactive Venus where the only seismicity on the planet is a background seismicity similar to the continental intraplate seismicity on Earth. This minimum level of seismicity on Venus is a popular hypothesis that has been used by other studies as well (e.g., Ganesh et al., 2023; Stevenson et al., 2015; Tian et al., 2023). Here we obtain this estimate by scaling the entirety of Venus with continental intraplate seismicity on Earth.

As a second estimate, we consider an active Venus with conservative assumptions on its level of activity to provide a lower bound. Following Byrne and Krishnamoorthy (2022), Davaille et al. (2017), and Gülcher et al. (2020), we assume that coronae are surface expressions of plume-lithosphere interactions with subduction-like features and therefore have a seismic signature similar to that of Earth's subduction zones. However, for this lower bound estimate, we do not consider the entire corona area to be active subduction-like features and associated with the high seismicity density of subduction zones. Instead, we assume that 27.8% of the area of coronae is active according to Gülcher et al. (2020) and we only scale this area with subduction zones on Earth. The remaining area of the coronae is scaled with continental intraplate seismicity on Earth. Hence, we effectively assume that the corona formation mechanism for the remaining coronae is more akin to seismicity associated with hot spots or delamination processes on Earth, whose seismic signatures are implicitly included in our continental and oceanic intraplate seismic densities for Earth. We further assume that the rift zones on Venus have seismicity similar to (continental) rift zones on Earth (Basilevsky & McGill, 2007; Foster & Nimmo, 1996; Graff et al., 2018; Harris & Bédard, 2015; Solomon, 1993). The observed fold belts on Venus that we assume to be compressional features are assumed to have a similar seismicity signature to collision zones on Earth. Like the inactive Venus scenario, the remaining area of Venus is scaled according to continental intraplate seismicity on Earth.

Our third and last estimate is for an active Venus with the most liberal assumptions of plausible tectonic activity on Venus. In this estimate, we assume that all coronae are active, since the amount of active coronae is still highly uncertain (Gülcher et al., 2020). So, we scale the entire corona area with the subduction seismicity of the Earth. For the rift zones on Venus, we now scale the seismicity with mid-oceanic ridge seismicity on Earth, instead of continental rifting (Graff et al., 2018). Like our lower bound estimate for active Venus, we scale the area of fold belts on Venus with collision zones on Earth and we assume that the rest of the planet is equivalent to continental intraplate seismicity on Earth.

Combining the scaling for the seismogenic zone thickness (Section 2.4.1) with the three scalings based on the tectonic features allows us to arrive at three different end-member seismicity estimates for Venus. In short, we obtain the global amount of annual venusquakes for a certain magnitude  $N_{\text{vq}|M_w}$  by applying the following equation:

$$N_{\text{vq}|M_w} = f_{\Delta D} \sum_{\text{tectonic features}} A_{t,V} \cdot \frac{N_{\text{eq},t|M_w}}{A_{t,E}} \quad (2)$$

where  $f_{\Delta D}$  is the seismogenic zone scaling factor (i.e., 0.27 and 0.84);  $A_{t,V}$  is the surface area  $A$  of a tectonic feature  $t$  on Venus  $V$ ;  $N_{\text{eq},t|M_w}$  is the number of annual earthquakes for a given analogous Earth tectonic feature at a given moment magnitude; and  $A_{t,E}$  is the corresponding surface area of the analogous tectonic feature on Earth. The sum then indicates a summation over all the tectonic features that are scaled to Venus, up to and including the intraplate regions, such that we sum over the entire surface area of Venus. Scaling with the seismogenic thickness as well as the areas of the tectonic settings, effectively allows us to scale by seismogenic volume per tectonic setting to obtain estimates for Venus' seismicity (Table S3 in Supporting Information S1).

### 2.4.3. Extrapolating to Other Magnitudes

In order to actually calculate the potential amount of venusquakes and to extrapolate to earthquake magnitudes below the completeness magnitude of  $M_w 5$  of the CMT catalog, we effectively scale the average slopes of the size-frequency distribution for the different tectonic settings on Earth (equivalent to  $N_{eq,t}$  for all moment magnitudes; Figure 1c). We specifically assume that the size-frequency distribution of medium-sized earthquakes with a seismic moment of  $10^{17}$  to  $10^{19}$  N m is representative for the size-frequency distribution of smaller earthquake magnitudes, that is, the earthquakes follow Gutenberg-Richter statistics (Beroza & Kanamori, 2015; Gutenberg & Richter, 1956). This assumption allows us to provide estimates of the amount of venusquakes with moment magnitudes of  $M_w 3$  and  $M_w 4$ . We refrain from reporting on the amount of venusquakes with lower magnitudes, because they are unlikely to be detected in future seismological exploration missions of Venus (Brissaud et al., 2021; Krishnamoorthy et al., 2020).

Note that this assumption means that we consider the same  $b$ -value averaged per  $\text{km}^2$  of the Earth analogs for the different tectonic settings of Venus. Moreover, we assume that this  $b$ -value is constant for all quake magnitudes. From seismic catalogs on Earth, we know this is not necessarily realistic as the frequency of earthquakes with  $M_w \geq 7$  starts to drop (Figure 1), although this could also be a result of the limited observational period of the current seismic catalogs (typically no more than  $\sim 100$  years). Since there is limited data for Earth on earthquakes with magnitudes  $\geq M_w 8$ , because of their large recurrence time (Figure 1), calculating the amount of large venusquakes with magnitudes  $\geq M_w 8$  is less straightforward than extrapolating to smaller quake magnitudes. In addition, the (potential) maximum quake magnitude on Venus is unknown. One contributing factor is the lower seismogenic thickness of Venus compared to Earth (Section 2.4.1), which affects the maximum magnitude of quakes and could potentially hint at a smaller maximum quake size on Venus than on Earth. For these reasons, we do not explicitly comment on the occurrence of quakes  $\geq M_w 8$  on Venus in this study, although our methodology does provide estimates (i.e., Figure 3). Considering the lower seismogenic thickness of Venus, and hence the smaller potential rupture area, we believe  $M_w 7$  venusquakes to be a reasonable first-order upper bound for our reporting on Venusian seismicity here.

## 3. Results

Our results for the different Venus scenarios are summarized in Figure 3 and Tables 1 and 2, where we list the estimated annual number of quakes for a given moment magnitude and the global seismicity densities on Venus for our different estimates.

### 3.1. Inactive Venus

In our first estimate, we assume that the entirety of Venus can be scaled with the continental intraplate seismicity of the Earth, so the global estimate and the intraplate estimate overlap perfectly in Figure 3b. As expected, the amount of seismicity in this scenario is significantly less than that on Earth with 95–296 venusquakes  $\geq M_w 4$  estimated annually, compared to 12,207 earthquakes  $\geq M_w 4$  per year on Earth. The associated seismicity density for quakes  $\geq M_w 4$  lies between  $0.21 \cdot 10^{-6}$  and  $0.64 \cdot 10^{-6} \text{ year}^{-1} \text{ km}^{-2}$  (Table 2), which is on the same order of magnitude as that of intraplate seismicity on Earth.

### 3.2. Active Venus—Lower Bound

The lower bound for our active Venus estimate globally predicts more seismicity than the inactive, intraplate Venus estimate (Section 3.1). The fold belt, rift, and intraplate tectonic settings on Venus have seismicity on the same order of magnitude in this estimate, as shown by the overlapping bands of seismicity in Figure 3c (also see Figure S1 in Supporting Information S1). The coronae have an order of magnitude more seismicity associated with them, although only 27.8% of them are assumed to have a subduction-like seismicity density in this estimate. Summing up the seismicity of the different tectonic settings results in estimates of 1,161–3,609 venusquakes per year with a moment magnitude  $\geq M_w 4$  and a seismicity density of  $2.52 \cdot 10^{-6}$  to  $7.84 \cdot 10^{-6} \text{ year}^{-1} \text{ km}^{-2}$  globally for venusquakes  $\geq M_w 4$  (Table 2). This global seismicity density is significantly less than that of the Earth or any of its plate boundary settings.

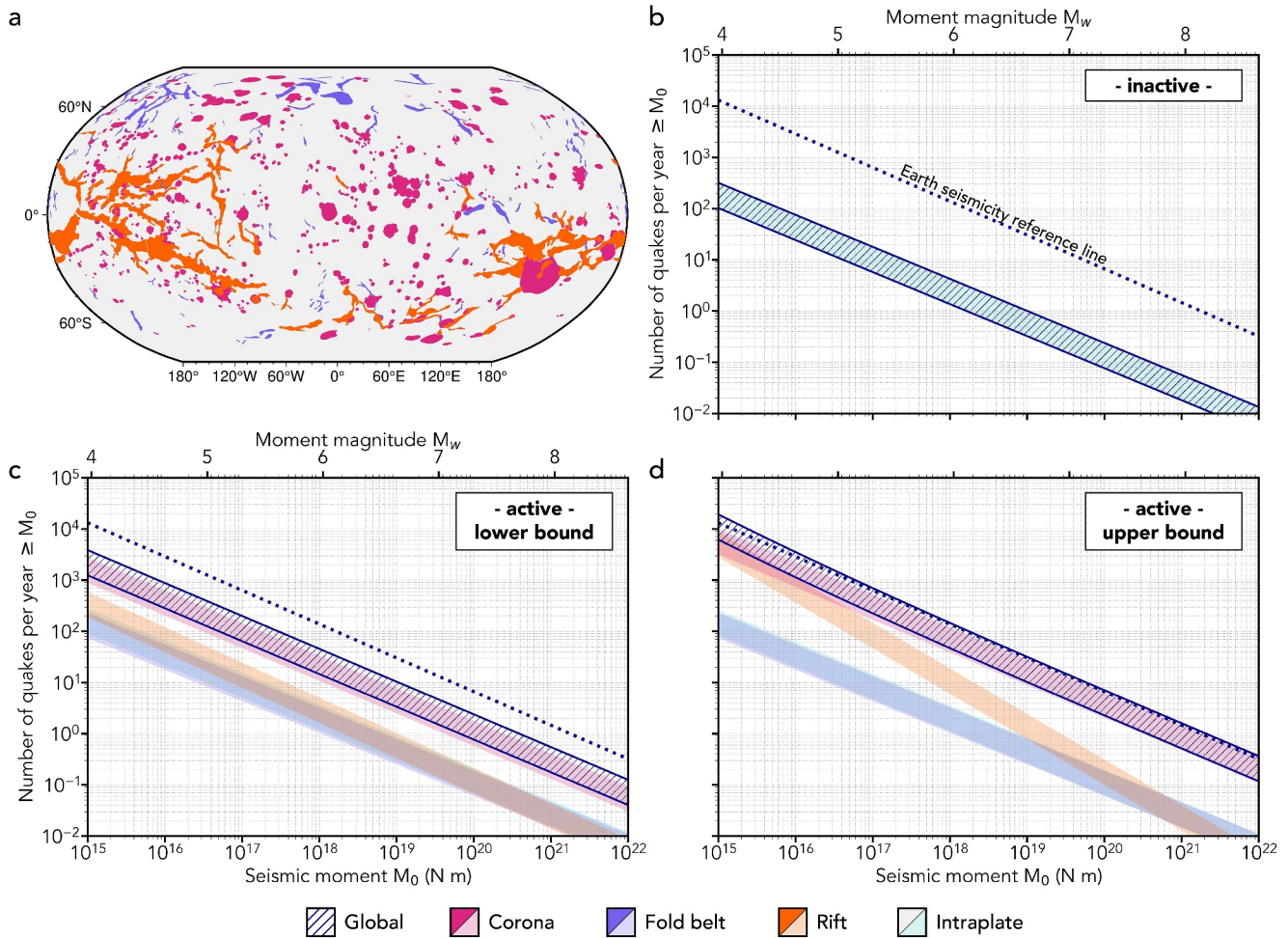


**Figure 3.** (a) Map of Venus (Robinson projection) showing the areas of mapped coronae, fold belts, and rifts (Price & Suppe, 1995; Price et al., 1996). (b–d) Ranges of potential quake size-frequency distributions on Venus for (b) an inactive Venus with background seismicity analogous to Earth’s continental intraplate seismicity; (c) a lower bound on an active Venus; and (d) an upper bound on an active Venus. The hatched area shows the global, accumulated annual seismicity that combines the seismicity of the different individual tectonic settings. Note that because of the log-log scale, the global estimate and the seismicity range of the highest individual tectonic setting are closely spaced. Dotted dark blue line indicates the reference Earth seismicity, which corresponds to the slope of the size-frequency distribution for seismic moments of  $10^{17}$  to  $10^{19}$  N m of global seismicity on Earth (Figure 1c).

### 3.3. Active Venus—Upper Bound

The upper bound of estimated seismicity for an active Venus (Figure 3d, Figure S2 in Supporting Information S1) is very close to the annual seismicity observed on Earth, primarily due to the scaling of coronae with Earth’s subduction zone seismicity in this estimate, which also dominates Earth’s seismicity (Figure 1c). Since we scale the rifts on Venus with Earth’s mid-oceanic ridge seismicity in this estimate, we have a different slope for Venusian rift seismicity. This results in an increase in smaller quakes with  $M_w \leq 5$ . There is no difference between

**Table 1**  
Number of Venusquakes per Year Equal to or Larger Than a Certain Moment Magnitude for Our Three Possible Venus Scenarios

Estimate	$M_w \geq 3.0$	$M_w \geq 4.0$	$M_w \geq 5.0$	$M_w \geq 6.0$	$M_w \geq 7.0$
Inactive Venus	826–2,568	95–296	11–34	1–4	0–0
Active Venus—lower bound	10,760–33,460	1,161–3,609	126–391	14–42	2–5
Active Venus—upper bound	84,263–262,023	5,715–17,773	465–1,446	44–136	4–15

Note. A range is provided based on the uncertainties in the chosen scaling factor for the seismogenic thickness.

**Table 2**

*Estimated Minimum and Maximum Seismicity Densities on Venus for Quakes  $\geq M_w 4$  for Three Scenarios With Different Activity-Level Assumptions*

Estimate	Minimum seismicity density ( $\cdot 10^{-6}$ year $^{-1}$ km $^{-2}$ )	Maximum seismicity density ( $\cdot 10^{-6}$ year $^{-1}$ km $^{-2}$ )
Inactive Venus	0.21	0.64
Active Venus—lower bound	2.52	7.84
Active Venus—upper bound	12.42	38.62

the seismicity expected for the fold belt tectonic setting compared to the lower bound for an active Venus (Section 3.2), as it is scaled in the same way.

Globally, we then estimate 5,715–17,773 venusquakes of moment magnitude  $\geq M_w 4$ , with the upper bound being larger than the number of  $M_w \geq 4$  earthquakes estimated for the Earth (12,207). However, note here that this estimate for the number of earthquakes with  $M_w \geq 4$  on Earth is an extrapolation of the CMT catalog, which has a completeness magnitude of  $M_w 5$ . Therefore, the number of earthquakes  $M_w \geq 4$  on Earth is potentially underestimated, leading to similar amounts of estimated seismicity for the upper bound estimate of Venus as on Earth. The seismicity density of quakes  $M_w \geq 4$  varies from  $12.42 \cdot 10^{-6}$  to  $38.62 \cdot 10^{-6}$  year $^{-1}$  km $^{-2}$  (Table 2). This lowest possible seismicity density of quakes  $M_w \geq 4$  for an upper bound to our active Venus estimate is slightly lower than the Earth's seismicity density of quakes  $M_w \geq 4$  for continental rift zones ( $16.98 \cdot 10^{-6}$  year $^{-1}$  km $^{-2}$ ) and the highest possible seismicity density of quakes  $M_w \geq 4$  is larger than that of the seismicity density of collision settings on the Earth ( $33.62 \cdot 10^{-6}$  year $^{-1}$  km $^{-2}$ ) (Table S1 in Supporting Information S1).

## 4. Discussion

In this study, we provide three end-member estimates of possible Venusian seismicity by looking at Earth analogs, following the same philosophy of Byrne and Krishnamoorthy (2022) who previously applied this logic to determine the frequency of volcanic eruptions on Venus. In contrast to Byrne and Krishnamoorthy (2022), we calculate the seismicity densities for individual tectonic settings and then scale according to their surface areas and appropriate Earth analogs.

Generally, we estimate that the seismicity of Venus is lower than that of the Earth, except for the most active end-member of Venus activity, which shows seismicity levels similar to that of present-day Earth (Figure 4). At the same time, even the lowest estimate of seismicity for an inactive Venus is larger than the estimated global seismicity of Mars by up to an order of magnitude and of the Moon by several orders of magnitude. The global estimates for these “tectonically dead,” stagnant-lid planets are based on extrapolations from measured seismicity by the InSight mission in the case of Mars (Giardini et al., 2020) and analysis of shallow moonquake activity for the Moon (Oberst, 1987) as calculated by Banerdt et al. (2020). This large difference in global seismicity between Mars, the Moon, and Venus is expected even when Venus is tectonically inactive because the difference in size of the planets alone results in significantly less expected events annually for the Moon and Mars. In addition, the Moon and Mars most likely have a much cooler interior than Venus at present due to their smaller size, again resulting in a less geologically active body today.

There are large differences between the end-member estimates of Venus' seismicity, indicating a range of possible seismic activity on Venus at present, depending on the many assumptions we are forced to make given the limited amount of data from Venus. In the following, we discuss the assumptions and limitations of our method and comment on how our understanding of the seismicity of Venus could increase with upcoming missions.

### 4.1. Likely Causes of Differences Between the Seismicity on Earth and Venus

Before we assess the individual assumptions we made to obtain our different estimates of Venusian seismicity, it is useful to assess the overarching assumption that Earth's seismicity can be scaled to Venus.

One of the biggest and most straightforward differences between the Earth and Venus is their different surface temperature. Since temperature plays a crucial role in seismicity through its control on the brittle-ductile transition (Gutscher & Peacock, 2003; Hyndman et al., 1997; Peacock & Hyndman, 1999; Scholz, 2019; Tichelaar & Ruff, 1993), it will have a large effect on the amount of seismicity that can occur. On a global scale, different surface temperatures can result in different tectonic regimes and deformation mechanisms (Foley et al., 2012;

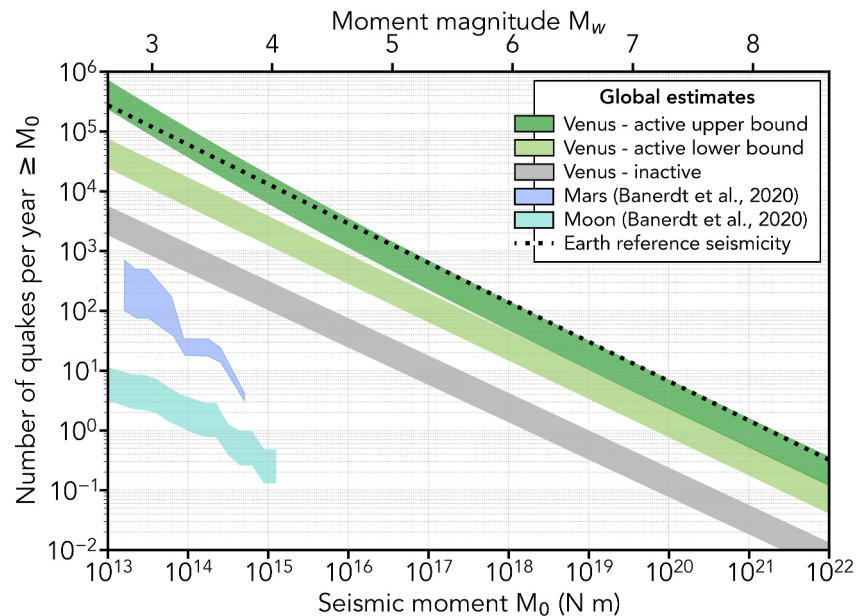


**Figure 4.** Summary of the global ranges of potential quake size-frequency distributions on Venus for our three end-member estimates from Figure 3. Global seismicity estimates for the Moon and Mars from Banerdt et al. (2020) are shown for reference. Dotted dark blue line indicates Earth's seismicity for reference, which corresponds to the slope of the size-frequency distribution of global seismicity on Earth for seismic moments of  $10^{17}$  to  $10^{19}$  N m (Figure 1c).

Lenardic et al., 2008; Weller et al., 2015) which could greatly change the seismic signatures. In its most extreme case some studies argue that there will be little to no seismicity on Venus, at least at higher magnitudes (e.g., Karato & Barbot, 2018). These studies argue that the high surface temperatures on Venus may exclude the possibility of any kind of substantial seismogenic zone and the unstable slip mechanisms responsible for earthquakes. Instead, the stresses that are built up in the Venusian lithosphere could be released through aseismic processes, such as creep (stable slip) and viscous flow. Karato and Barbot (2018) arrive at this conclusion by assuming a crustal thickness of 30 km based on a global stagnant lid regime and a limit of the seismogenic zone in the crust at the  $400^{\circ}\text{C}$  isotherm and in mantle at  $600^{\circ}\text{C}$ . However, recent estimates of the average crustal thickness of Venus are 15–20 km (James et al., 2013; Maia & Wiczorek, 2022). Additionally, strictly separating the mechanical behavior of the crust and mantle like this is unrealistic. Instead, a better approach might be to look at the behavior of the lithosphere as a whole. For oceanic lithosphere the limiting temperatures for the deepest quakes are the  $600\text{--}800^{\circ}\text{C}$  isotherms (Chen & Molnar, 1983). Applying these assumptions instead, the method of Karato and Barbot (2018) does predict a thin seismogenic layer with the possibility for quakes on Venus.

In contrast to this, there are also studies that cite the high surface temperature on Venus as a potential indirect source of quakes on Venus. Lognonné and Johnson (2015) mention that the rising surface temperature throughout Venus' evolution could generate compressive thermoelastic stresses in the crust (Dragoni & Piombo, 2003; Solomon et al., 1999). This increase in compressive stress could in turn form or activate reverse faults in Venus' lithosphere. Comparing to the Earth analogs of regions with compressive faulting, Lognonné and Johnson (2015) suggest that these stresses could lead to quakes with a maximum moment magnitude of 6.5.

The difference in surface temperature and hence temperature structure in the lithosphere could also change the shear modulus of the Venusian rocks compared to their terran counterparts. As the seismic moment of a quake depends on the shear modulus of the rocks, this could alter the magnitudes of quakes on Venus compared to Earth. As such, it could affect the size-frequency distribution of quakes and hence the  $b$ -value.

In our estimates, we have taken the difference in surface temperature and its effect on seismicity into account through scaling end-member estimates of the seismogenic thickness of Venus with the average seismogenic thickness of Earth. This implicitly assumes that the material properties, including the shear modulus, of rocks on Venus are the same as on Earth. Since the material properties of Venus' (near-)surface rocks are still very unconstrained with the scarce data that is available pointing toward Earth-like mid-oceanic ridge basaltic

compositions (e.g., Abdrakhimov & Basilevsky, 2002), we believe this is a reasonable assumption. At the very least, our approach presents a first-order approximation to take the difference in surface temperatures between the two planets into account, although it is by no means a perfect solution that encapsulates the true complexity of the effect of increased surface temperatures on seismicity on Venus.

Another important difference between Venus and Earth is likely to be the amount of water available in the crust. On Earth, water plays a vital role, especially in subduction seismicity, with the pore-fluid pressure crucial in determining the stresses in megathrust settings (Angiboust et al., 2012; Seno, 2009) and dehydration reactions responsible for intermediate-depth and deep seismicity in subduction zones (Green & Houston, 1995; Hacker et al., 2003; Houston, 2015; Jung et al., 2004; Wang et al., 2017). This water is typically added to the subduction system at the outer rise that underlies an ocean in subduction zones (Boneh et al., 2019). On Venus, the amount of water in the lithosphere is relatively unconstrained (Gillmann et al., 2022; Rolf et al., 2022), with some studies suggesting that Venus is currently relatively dry (Grinspoon, 1993; Namiki & Solomon, 1998; Salvador et al., 2022; Smrekar & Sotin, 2012), while others argue that there might still be a significant amount of water in Venus' mantle (Gillmann et al., 2022). This makes it highly uncertain how big a role water could play in the seismicity of Venus. Our estimates encompass the full spectrum of possible seismicity on Venus with our lower bound using Earth's intraplate seismicity, where water likely plays a smaller role, and our upper bound including subduction seismicity, where water is an important factor.

Strain rates play an important role in seismicity as well, because they determine the time scale of stress build-up and the recurrence time of earthquakes. On Venus, strain rates similar to Earth's active margins have been suggested by Grimm (1994). However, due to the lack of Earth-like plate tectonics and plate boundaries, there are overall potentially less large rupture areas, leading to less large-magnitude quakes on Venus. The decreased seismogenic thickness of Venus also plays a role in this by limiting the maximum rupture area. Although our estimates provide a range of potential venusquakes at large magnitudes (Table 1), it is therefore uncertain if large venusquakes could actually occur. Preliminary mission designs suggest that quake magnitudes of  $M_w \geq 3$  could be feasibly observed by a range of plausible seismic detection methods (Brissaud et al., 2021; Garcia et al., 2024; Krishnamoorthy et al., 2020) and our estimates are likely most plausible for this range of seismic magnitude  $3 \leq M_w \leq 5$ .

All in all, there are many uncertainties when it comes to estimating the seismicity of Venus from Earth's seismicity. Higher resolution data and missions focused on observing seismicity (discussed in Section 4.3) will help to obtain seismicity estimates for Venus independent of Earth. However, since those constraints are not yet available, scaling the seismicity of the Earth is a reasonable first-order approximation to gain some insights into the potential seismicity of Venus.

## 4.2. Assumptions in and Limitations of Our Seismicity Estimates

In order to provide global end-member ranges of the potential seismicity of Venus, one important simplification that we use is the constant global end-member seismogenic thickness (see Section 2.4.1). This assumption serves its purpose in that we obtain a range of plausible seismicity for each end-member estimate, but in reality, the seismogenic thickness will vary laterally across the surface of Venus and depend greatly on, for instance, the specific tectonic setting. Hence, in order to obtain more regionally accurate seismicity estimates, future studies should take into account laterally varying seismogenic thicknesses.

For our inactive Venus estimate, we assume that the global background seismicity of Venus is similar to the continental intraplate seismicity of the Earth. This is a common assumption that has also been suggested by for example, Byrne et al. (2021), Lorenz (2012), Stevenson et al. (2015), and Tian et al. (2023). The number of venusquakes  $\geq M_w 4$  per year for this estimate (95–296) is also the same order of magnitude as the estimate of Ganesh et al. (2023), who calculate an estimate of Venus' seismicity based on the cooling of the planet and the corresponding contraction of the lithosphere and thereby predict  $\sim 265$  venusquakes  $\geq M_w 4$  per year. Lognonné and Johnson (2015) mention that Stofan et al. (1993) arrive at a slightly higher estimate of 100 quakes  $\geq M_w 5$  per year for intraplate activity with a strain rate of  $10^{-19} \text{ s}^{-1}$  (Grimm & Hess, 1997). In comparison, we estimate 11–34 quakes  $\geq M_w 5$  per year. The reason for this discrepancy is that Stofan et al. (1993) assume a thicker seismogenic layer (30 km) than we do.

Of course, we cannot completely exclude a completely inactive Venus with seismicity densities even lower than our inactive Venus estimate. So, if future missions (Section 4.3) would find less than 95 quakes  $\geq M_w 4$  per year, this would indicate that either the processes that are responsible for creating intraplate seismicity on the Earth do not operate on Venus or the seismic moment release on Venus is fundamentally slower than on Earth. Physically, this lower seismic activity could for example be caused by the slower cooling of Venus than previously thought, thereby decreasing the amount of quakes predicted by Ganesh et al. (2023).

For our estimates for an active Venus, we scale the areas of fold belts associated with compressional deformation on Venus with the seismicity of collision zones on Earth. We believe this to be a reasonable assumption, considering that Venus' fold belts and the Earth analog are both compressional regimes. The rifts on Venus are scaled with continental rift seismicity on Earth in the lower bound estimate for an active Venus. This is also a reasonable assumption, with many studies pointing to the morphological and geological similarities between the rift zones on Venus and continental rifts on Earth such as the Eastern African rift zone (Basilevsky & McGill, 2007; Foster & Nimmo, 1996; Graff et al., 2018; Kiefer & Swafford, 2006; Regorda et al., 2023; Solomon, 1993; Stoddard & Jurdy, 2012). For our upper bound, we scale the rift zones of Venus with mid-oceanic ridge seismicity since it is also an extensional setting and the higher temperatures at the mid-oceanic ridges and the corresponding different slope of the size-frequency distribution on Earth might be a better fit for rift seismicity under Venus' high surface temperature. On Earth, the different seismic signatures between continental rifts and mid-oceanic ridges are not purely temperature-related. Instead, the inherent tectonic differences between the two settings plays a role as well. Since it is unclear which of these two physical mechanisms (or their seismic signatures) best represents the rifting processes on Venus, we believe using one of them for the lower bound estimate and one for the upper bound estimate catches the uncertainty in governing mechanisms in our estimates. For the coronae, we scale with subduction, since multiple studies suggest that coronae, or at least a subset of them, could be the surface expressions of plume-lithosphere interactions with subduction-like features (Byrne & Krishnamoorthy, 2022; Davaille et al., 2017; Gülcher et al., 2020). However, the seismicity associated with this type of plume-lithosphere interactions is uncertain. Assigning the same seismicity density as regular subduction processes on Earth follows Gülcher et al. (2020) and is a reasonable first-order approximation in the absence of other constraints, although the presumable lack of water in coronae and the higher surface temperature will certainly affect its seismic signature as well. Future modeling studies that combine geodynamic modeling with seismic cycle modeling and dynamic ruptures (e.g., van Dinther, Gerya, Dalguer, Corbi, et al., 2013; van Dinther, Gerya, Dalguer, Mai, et al., 2013; van Dinther et al., 2014; Van Zelst et al., 2019) are needed to assess the seismic signatures that could be expected at Venusian coronae. In the interest of providing an upper and lower bound, scaling the coronae by activity is a good first order approximation. However, it is also possible that coronae seismicity does not scale with Earth's subduction seismicity, but is instead more analogous to, for example, rift or transform fault seismicity, as suggested for the center of Artemis corona (Spencer, 2001). In general though, our upper bound for Venusian seismicity results in seismicity levels slightly higher than, but similar to, that of the Earth, which has also already been suggested previously (e.g., Lorenz, 2012). Choosing a different seismicity density for coronae, such as that of the transform fault setting, would result in a lower amount of estimated venusquakes. Since we are attempting to provide an upper limit to the possible amount of annual venusquakes, our assumption of a subduction seismicity density is reasonable.

Apart from the uncertainty in scaling the chosen tectonic settings correctly, there are also tectonic settings on Venus that we neglect to scale explicitly. For example, we do not explicitly scale the tesserae of Venus with a tectonic setting on Earth, although they are implicitly scaled with the background intracontinental seismicity of the Earth. This is arguably one of the most reasonable assumptions for tesserae, considering that prevailing hypotheses include that they are continental crust analogs (Gilmore et al., 2015; Romeo & Turcotte, 2008). We also do not consider the observed extensive regions of wrinkle ridges as seismically active beyond the background intracontinental seismicity of the Earth. A recent study by Sabbeth et al. (2023a) presented a conservative estimate of  $9.1 \cdot 10^{16}$  to  $5.1 \cdot 10^{17}$  N m per year for the annual moment release for wrinkle ridges on Venus based on (low-resolution) mapped fault lengths. Translating this to the size-frequency distributions we use here, Sabbeth et al. (2023a) estimate roughly one venusquake  $\geq M_w 4$  every 10 years, indicating that the seismicity of wrinkle ridges probably does not significantly contribute to the global seismic budget of the planet. Beyond tesserae and wrinkle ridges, there are also other kinds of deformation structures and potential seismic sources that are not directly considered in this study, such as densely fractured plains, that could also contribute to the seismicity of Venus.

Note that in the estimates presented here, only one type of seismic source is considered, that is, earthquakes, which by definition are associated with tectonics and volcanism. Other sources such as landslides (Bulmer, 2012; Bulmer & Guest, 1996; Bulmer et al., 2006; Hahn & Byrne, 2023; Pavri et al., 1992) could be responsible for seismic signals on Venus as well.

### 4.3. Determining the Actual Seismicity of Venus in the Future

In the next decade, VERITAS (Smrekar et al., 2020) and EnVision (Ghail et al., 2016) will provide a wealth of new data, including high resolution topography, that will provide better constraints on the actual lengths, offsets, and displacements of Venusian faults. This will provide another basis of estimating Venus' seismicity through scaling relationships applied to surface fault observations (Sabbeth et al., 2023a, 2023b).

The new Venus missions will also indirectly provide stronger constraints on the seismogenic thickness, which is typically deduced from thermal gradients estimated from studies of the elastic and mechanical lithosphere thickness (e.g., Anderson & Smrekar, 2006; Borrelli et al., 2021; Maia & Wiczorek, 2022; Smrekar et al., 2023) or from impact crater modeling (Bjornes et al., 2021). These studies rely on the analysis of gravity and topography data, for which a higher resolution will become available from the VERITAS (Smrekar et al., 2020) and EnVision (Ghail et al., 2016) missions. Estimates of the thermal gradient and associated seismogenic thickness could then be obtained with a higher accuracy and on a more global scale than currently available. They could be included in future studies of seismicity on Venus and improve on the estimates presented here.

Most importantly though, VERITAS will be able to directly measure surface deformation through Repeat Pass Interferometry (RPI) at 2 cm height precision (Smrekar et al., 2020). Resources permitting, EnVision also hopes to conduct RPI measurements in its extended mission. Besides quantifying movements on the surface of Venus for the first time, both missions will also qualitatively provide insights into which regions are geologically and potentially seismically active.

Until the era of new Venus data, we are unfortunately limited by the currently available data sets. The simplest, first-order estimate of the seismicity of Venus is therefore obtained here through scaling Earth analogs to Venus, without considering individual fault lengths or displacements and detailed seismogenic thickness estimates and instead uses the seismicity density characteristics of different tectonic settings on Earth.

To distinguish between the different scenarios presented in this study and determine how seismically active Venus is, a seismological or geophysical mission to Venus is required to measure seismic signals (Garcia et al., 2024). Although the NASA- and ESA-selected missions to Venus currently do not focus on this, there are promising proposals to measure Venus' seismicity in the not-too-distant future. For example, Kremic et al. (2020) presented a mission proposal for a long-duration Venus lander with a seismometer on board that can withstand Venus' high surface temperature. In addition, recent advances in the balloon-detection of earthquakes show great promise for applications to Venus (Garcia et al., 2022; Krishnamoorthy & Bowman, 2023). Our estimates for Venusian seismicity may help guide the design of these missions.

## 5. Conclusions

We estimate upper and lower bounds on the expected annual seismicity of Venus by scaling the seismicity of the Earth to Venus according to the surface area of different tectonic settings and the difference in seismogenic thickness between the two planets. Our most conservative estimate is an “inactive Venus,” where we assume that the global seismicity of Venus is comparable to Earth's continental intraplate seismicity. This results in 95–296 venusquakes  $\geq M_w 4$  per year depending on the assumption of seismogenic zone thickness. For our active Venus scenarios, we assume that the rifts, fold belts, and coronae on Venus are seismically active. For a lower bound on an active Venus, we then find 1,161–3,609 venusquakes  $\geq M_w 4$  annually, which increases to 5,715–17,773 venusquakes  $\geq M_w 4$  for assumptions that constitute our most active Venus scenario. The upper bound of this latter scenario is similar to the seismic activity level of the Earth. Future seismological and geophysical missions could measure the actual seismicity of Venus and distinguish between our three proposed end-members of Venusian seismic activity.



## Data Availability Statement

The Jupyter Notebooks used to make the results and plot the figures as well as the CMT database and geospatial vector data (shapefiles) of the tectonic setting areas on Earth and Venus can be found in Van Zelst et al. (2024). Explanations of individual files in this repository and additional figures and tables are provided in Supporting Information S1. The Venus mapping data used here from Price and Suppe (1995) and Price et al. (1996) can also be found in the ArcGIS repository “Venus Geology and Tectonics” at <https://www.arcgis.com/home/item.html?id=962dcfd6b5b64b21a922bc9b6c94ad78>. The topography maps were created using the VenusTopo719 data set (Wieczorek, 2015) and the radar image mosaics can be found in Pettengill (1992). Figures were made with Python in Jupyter Notebooks and Adobe Illustrator. We used the colorblind-friendly color map from the IBM Design Library (Nichols, 2022; retrieved: 16 February 2023).

## Acknowledgments

We warmly thank editor Laurent Montési and reviewers Sue Smrekar, Joseph O'Rourke, and Angela Marusiak who provided thorough and constructive feedback. We also thank two anonymous reviewers who provided feedback on an earlier version submitted to GRL. This research was supported by the International Space Science Institute (ISSI) in Bern, Switzerland through ISSI International Team project #566: Seismicity on Venus: Prediction & Detection. The authors warmly thank the entire ISSI team for fruitful discussions and feedback. IvZ, JSM, ACP, and MS additionally acknowledge the financial support and endorsement from the DLR Management Board Young Research Group Leader Program and the Executive Board Member for Space Research and Technology. IvZ also gratefully acknowledges the support by the Deutsche Forschungsgemeinschaft (DFG, German Research Foundation), Project-ID 263649064—TRR 170. Open Access funding enabled and organized by Projekt DEAL.

## References

- Abdrakhimov, A., & Basilevsky, A. (2002). Geology of the Venera and Vega landing-site regions. *Solar System Research*, 36(2), 136–159. <https://doi.org/10.1023/a:1015222316518>
- Aderhold, K., & Abercrombie, R. E. (2016). Seismotectonics of a diffuse plate boundary: Observations off the Sumatra-Andaman trench. *Journal of Geophysical Research: Solid Earth*, 121(5), 3462–3478. <https://doi.org/10.1002/2015jb012721>
- Ágústsson, K., & Flóvenz, Ó. G. (2005). The thickness of the seismogenic crust in Iceland and its implications for geothermal systems. In *Proceedings of the world geothermal congress* (pp. 24–29).
- Anderson, F. S., & Smrekar, S. E. (2006). Global mapping of crustal and lithospheric thickness on Venus. *Journal of Geophysical Research*, 111(E8), E08006. <https://doi.org/10.1029/2004je002395>
- Angiboust, S., Wolf, S., Burov, E., Agard, P., & Yamato, P. (2012). Effect of fluid circulation on subduction interface tectonic processes: Insights from thermo-mechanical numerical modelling. *Earth and Planetary Science Letters*, 357, 238–248. <https://doi.org/10.1016/j.epsl.2012.09.012>
- Baes, M., Stern, R. J., Whattam, S., Gerya, T. V., & Sobolev, S. V. (2021). Plume-induced subduction initiation: Revisiting models and observations. *Frontiers in Earth Science*, 9, 766604. <https://doi.org/10.3389/feart.2021.766604>
- Banerdt, W. B., Smrekar, S. E., Banfield, D., Giardini, D., Golombek, M., Johnson, C. L., et al. (2020). Initial results from the InSight mission on Mars. *Nature Geoscience*, 13(3), 183–189. <https://doi.org/10.1038/s41561-020-0544-y>
- Basilevsky, A. T., & Head, J. W. (1997). Onset time and duration of corona activity on Venus: Stratigraphy and history from photogeologic study of stereo images. *Earth, Moon, and Planets*, 76(1), 67–115. <https://doi.org/10.1023/a:1006009531826>
- Basilevsky, A. T., & McGill, G. E. (2007). Surface evolution of Venus. In *Exploring Venus as a terrestrial planet* (Vol. 176, pp. 23–43). <https://doi.org/10.1029/176GM04>
- Beroza, G., & Kanamori, H. (2015). 4.01 - Earthquake seismology: An introduction and overview. In G. Schubert (Ed.), *Treatise on geophysics* (2nd ed., pp. 1–50). Elsevier. <https://doi.org/10.1016/B978-0-444-53802-4.00069-5>
- Bjornnes, E., Johnson, B., & Evans, A. (2021). Estimating Venusian thermal conditions using multiring basin morphology. *Nature Astronomy*, 5(5), 498–502. <https://doi.org/10.1038/s41550-020-01289-6>
- Boettcher, M. S., Hirth, G., & Evans, B. (2007). Olivine friction at the base of oceanic seismogenic zones. *Journal of Geophysical Research*, 112(B1), B01205. <https://doi.org/10.1029/2006jb004301>
- Boneh, Y., Schottenfels, E., Kwong, K., Van Zelst, I., Tong, X., Eimer, M., et al. (2019). Intermediate-depth earthquakes controlled by incoming plate hydration along bending-related faults. *Geophysical Research Letters*, 46(7), 3688–3697. <https://doi.org/10.1029/2018GL01585>
- Borrelli, M. E., O'Rourke, J. G., Smrekar, S. E., & Ostberg, C. M. (2021). A global survey of lithospheric flexure at steep-sided domical volcanoes on Venus reveals intermediate elastic thicknesses. *Journal of Geophysical Research: Planets*, 126(7), e2020JE006756. <https://doi.org/10.1029/2020je006756>
- Brissaud, Q., Krishnamoorthy, S., Jackson, J. M., Bowman, D. C., Komjathy, A., Cutts, J. A., et al. (2021). The first detection of an earthquake from a balloon using its acoustic signature. *Geophysical Research Letters*, 48(12), e2021GL093013. <https://doi.org/10.1029/2021gl093013>
- Brossier, J., Gilmore, M. S., & Head, J. W. (2022). Extended rift-associated volcanism in Ganis Chasma, Venus detected from Magellan radar emissivity. *Geophysical Research Letters*, 49(15), e2022GL099765. <https://doi.org/10.1029/2022gl099765>
- Bulmer, M. H. K., & Guest, J. (1996). Modified volcanic domes and associated debris aprons on Venus. *Geological Society, London, Special Publications*, 110(1), 349–371. <https://doi.org/10.1144/gsl.sp.1996.110.01.25>
- Bulmer, M. H. K., Petley, D., Murphy, W., & Mantovani, F. (2006). Detecting slope deformation using two-pass differential interferometry: Implications for landslide studies on Earth and other planetary bodies. *Journal of Geophysical Research*, 111(E6), E06S16. <https://doi.org/10.1029/2005je002593>
- Bulmer, M. H. K. (2012). Landslides on other planets. In J. J. Clague & D. Stead (Eds.), *Landslides: Types, mechanisms and modeling* (pp. 393–408). Cambridge University Press. <https://doi.org/10.1017/CBO9780511740367.033>
- Byrne, P. K., Ghail, R. C., Şengör, A. C., James, P. B., Klimczak, C., & Solomon, S. C. (2021). A globally fragmented and mobile lithosphere on Venus. *Proceedings of the National Academy of Sciences*, 118(26), e2025919118. <https://doi.org/10.1073/pnas.2025919118>
- Byrne, P. K., & Krishnamoorthy, S. (2022). Estimates on the frequency of volcanic eruptions on Venus. *Journal of Geophysical Research: Planets*, 127(1), e2021JE007040. <https://doi.org/10.1029/2021je007040>
- Chen, W.-P., & Molnar, P. (1983). Focal depths of intracontinental and intraplate earthquakes and their implications for the thermal and mechanical properties of the lithosphere. *Journal of Geophysical Research*, 88(B5), 4183–4214. <https://doi.org/10.1029/jb088ib05p04183>
- Davaille, A., Smrekar, S. E., & Tomlinson, S. (2017). Experimental and observational evidence for plume-induced subduction on Venus. *Nature Geoscience*, 10(5), 349–355. <https://doi.org/10.1038/ngeo2928>
- Dombard, A. J., Johnson, C. L., Richards, M. A., & Solomon, S. C. (2007). A magmatic loading model for coronae on Venus. *Journal of Geophysical Research*, 112(E4), E04006. <https://doi.org/10.1029/2006je002731>
- Dragoni, M., & Piombo, A. (2003). A model for the formation of wrinkle ridges in volcanic plains on Venus. *Physics of the Earth and Planetary Interiors*, 135(2–3), 161–171. [https://doi.org/10.1016/s0031-9201\(02\)00205-4](https://doi.org/10.1016/s0031-9201(02)00205-4)
- Dyar, M. D., Helbert, J., Cooper, R. F., Sklute, E. C., Maturilli, A., Mueller, N. T., et al. (2021). Surface weathering on Venus: Constraints from kinetic, spectroscopic, and geochemical data. *Icarus*, 358, 114139. <https://doi.org/10.1016/j.icarus.2020.114139>

- Dziewonski, A. M., Chou, T.-A., & Woodhouse, J. H. (1981). Determination of earthquake source parameters from waveform data for studies of global and regional seismicity. *Journal of Geophysical Research*, *86*(B4), 2825–2852. <https://doi.org/10.1029/jb086ib04p02825>
- Ekström, G., Nettles, M., & Dziewoński, A. (2012). The global CMT project 2004–2010: Centroid-moment tensors for 13,017 earthquakes. *Physics of the Earth and Planetary Interiors*, *200*, 1–9. <https://doi.org/10.1016/j.pepi.2012.04.002>
- Emmerson, B., & McKenzie, D. (2007). Thermal structure and seismicity of subducting lithosphere. *Physics of the Earth and Planetary Interiors*, *163*(1–4), 191–208. <https://doi.org/10.1016/j.pepi.2007.05.007>
- Filiberto, J., Trang, D., Treiman, A. H., & Gilmore, M. S. (2020). Present-day volcanism on Venus as evidenced from weathering rates of olivine. *Science Advances*, *6*(1), eaax7445. <https://doi.org/10.1126/sciadv.aax7445>
- Foley, B. J., Bercovici, D., & Landuyt, W. (2012). The conditions for plate tectonics on super-Earths: Inferences from convection models with damage. *Earth and Planetary Science Letters*, *331*, 281–290. <https://doi.org/10.1016/j.epsl.2012.03.028>
- Foster, A., & Nimmo, F. (1996). Comparisons between the rift systems of East Africa, Earth and Beta Regio, Venus. *Earth and Planetary Science Letters*, *143*(1–4), 183–195. [https://doi.org/10.1016/0012-821X\(96\)00146-X](https://doi.org/10.1016/0012-821X(96)00146-X)
- Frank, S. L., & Head, J. W. (1990). Ridge belts on Venus: Morphology and origin. *Earth, Moon, and Planets*, *50*(1), 421–470. <https://doi.org/10.1007/bf00142402>
- Ganesh, I., Herrick, R. R., & Kremic, T. (2023). Bounds on Venus's seismicity from theoretical and analog estimations. In *LPSC abstracts, No. 2806*. Retrieve from <https://ui.adsabs.harvard.edu/abs/2023LPICo2806.1851G>
- García, R. F., Klotz, A., Hertzog, A., Martin, R., Gérier, S., Kassarian, E., et al. (2022). Infrasound from large earthquakes recorded on a network of balloons in the stratosphere. *Geophysical Research Letters*, *49*(15), e2022GL098844. <https://doi.org/10.1029/2022gl098844>
- García, R. F., van Zelst, I., Kawamura, T., Näsholm, S. P., Horleston, A. C., Klaasen, S., et al. (2024). Seismic wave detectability on Venus using ground deformation sensors, infrasound sensors on balloons and airglow imagers. *ESS Open Archive*. <https://doi.org/10.22541/essoar.171286367.76819789/v1>
- Gerya, T. V. (2014). Plume-induced crustal convection: 3D thermomechanical model and implications for the origin of novae and coronae on Venus. *Earth and Planetary Science Letters*, *391*, 183–192. <https://doi.org/10.1016/j.epsl.2014.02.005>
- Ghail, R., Wilson, C. F., & Widemann, T. (2016). EnVision M5 Venus orbiter proposal: Opportunities and challenges. In *AAS/division for planetary sciences meeting abstracts# 48* (Vol. 48, pp. 216–308). Retrieved from <https://ui.adsabs.harvard.edu/abs/2016DPS....4821608G>
- Giardini, D., Lognonné, P., Banerdt, W. B., Pike, W. T., Christensen, U., Ceylan, S., et al. (2020). The seismicity of Mars. *Nature Geoscience*, *13*(3), 205–212. <https://doi.org/10.1038/s41561-020-0539-8>
- Gillmann, C., Way, M. J., Avicé, G., Breuer, D., Golabek, G. J., Höning, D., et al. (2022). The long-term evolution of the atmosphere of Venus: Processes and feedback mechanisms: Interior-exterior exchanges. *Space Science Reviews*, *218*(7), 56. <https://doi.org/10.1007/s11214-022-00924-0>
- Gilmore, M. S., Mueller, N., & Helbert, J. (2015). VIRTIS emissivity of Alpha Regio, Venus, with implications for tessera composition. *Icarus*, *254*, 350–361. <https://doi.org/10.1016/j.icarus.2015.04.008>
- Gilmore, M. S., Darby Dyar, M., Mueller, N., Brossier, J., Santos, A. R., Ivanov, M., et al. (2023). Mineralogy of the Venus surface. *Space Science Reviews*, *219*(7), 52. <https://doi.org/10.1007/s11214-023-00988-6>
- Golombek, M. P., Banerdt, W. B., Tanaka, K. L., & Tralli, D. M. (1992). A prediction of Mars seismicity from surface faulting. *Science*, *258*(5084), 979–981. <https://doi.org/10.1126/science.258.5084.979>
- Graff, J., Ernst, R. E., & Samson, C. (2018). Evidence for triple-junction rifting focussed on local magmatic centres along Parga Chasma, Venus. *Icarus*, *306*, 122–138. <https://doi.org/10.1016/j.icarus.2018.02.010>
- Green, H. W., & Houston, H. (1995). The mechanics of deep earthquakes. *Annual Review of Earth and Planetary Sciences*, *23*(1), 169–213. <https://doi.org/10.1146/annurev.ea.23.050195.001125>
- Grimm, R. E., & Hess, P. (1997). The crust of Venus. In *Venus II: Geology, geophysics, atmosphere, and solar wind environment* (p. 1205). Retrieved from [muse.jhu.edu/book/98963](https://muse.jhu.edu/book/98963)
- Grimm, R. E. (1994). Recent deformation rates on Venus. *Journal of Geophysical Research*, *99*(E11), 23163–23171. <https://doi.org/10.1029/94je02196>
- Grindrod, P. M., & Hoogenboom, T. (2006). Venus: The corona conundrum. *Astronomy & Geophysics*, *47*(3), 3–16. <https://doi.org/10.1111/j.1468-4004.2006.47316.x>
- Grinspoon, D. H. (1993). Implications of the high D/H ratio for the sources of water in Venus' atmosphere. *Nature*, *363*(6428), 428–431. <https://doi.org/10.1038/363428a0>
- Gülcher, A. J., Gerya, T. V., Montési, L. G., & Munch, J. (2020). Corona structures driven by plume–lithosphere interactions and evidence for ongoing plume activity on Venus. *Nature Geoscience*, *13*(8), 547–554. <https://doi.org/10.1038/s41561-020-0606-1>
- Gülcher, A. J., Yu, T.-Y., & Gerya, T. V. (2023). Tectono-magmatic evolution of asymmetric coronae on Venus: Topographic classification and 3D thermo-mechanical modeling. *Journal of Geophysical Research: Planets*, *128*(11), e2023JE007978. <https://doi.org/10.1029/2023je007978>
- Gutenberg, B., & Richter, C. F. (1956). Magnitude and energy of earthquakes. *Annals of Geophysics*, *9*(1), 1–15. <https://doi.org/10.1038/176795a0>
- Gutscher, M.-A., & Peacock, S. M. (2003). Thermal models of flat subduction and the rupture zone of great subduction earthquakes. *Journal of Geophysical Research*, *108*(B1), ESE-2. <https://doi.org/10.1029/2001jb000787>
- Hacker, B. R., Peacock, S. M., Abers, G. A., & Holloway, S. D. (2003). Subduction factory 2. Are intermediate-depth earthquakes in subducting slabs linked to metamorphic dehydration reactions? *Journal of Geophysical Research*, *108*(B1), 2030. <https://doi.org/10.1029/2001jb001129>
- Hahn, R. M., & Byrne, P. K. (2023). A morphological and spatial analysis of volcanoes on Venus. *Journal of Geophysical Research: Planets*, *128*(4), e2023JE007753. <https://doi.org/10.1029/2023je007753>
- Harris, L. B., & Bédard, J. H. (2015). Interactions between continent-like 'drift', rifting and mantle flow on Venus: Gravity interpretations and Earth analogues. *Geological Society, London, Special Publications*, *401*(1), 327–356. <https://doi.org/10.1144/sp401.9>
- Hasterok, D., Halpin, J. A., Collins, A. S., Hand, M., Kreemer, C., Gard, M. G., & Glorie, S. (2022). New maps of global geological provinces and tectonic plates. *Earth-Science Reviews*, *231*, 104069. <https://doi.org/10.1016/j.earscirev.2022.104069>
- He, C., Wang, Z., & Yao, W. (2007). Frictional sliding of gabbro gouge under hydrothermal conditions. *Tectonophysics*, *445*(3–4), 353–362. <https://doi.org/10.1016/j.tecto.2007.09.008>
- Head, J. W. (1990). Venus trough-and-ridge tessera: Analog to Earth oceanic crust formed at spreading centers? *Journal of Geophysical Research*, *95*(B5), 7119–7132. <https://doi.org/10.1029/jb095ib05p07119>
- Herrick, R. R. (1999). Small mantle upwellings are pervasive on Venus and Earth. *Geophysical Research Letters*, *26*(6), 803–806. <https://doi.org/10.1029/1999gl900063>
- Herrick, R. R., Bjonnes, E. T., Carter, L. M., Gerya, T., Ghail, R. C., Gillmann, C., et al. (2023). Resurfacing history and volcanic activity of Venus. *Space Science Reviews*, *219*(4), 29. <https://doi.org/10.1007/s11214-023-00966-y>

- Herrick, R. R., & Hensley, S. (2023). Surface changes observed on a Venusian volcano during the Magellan mission. *Science*, 379(6638), 1205–1208. <https://doi.org/10.1126/science.abm7735>
- Hoogenboom, T., & Houseman, G. A. (2006). Rayleigh–Taylor instability as a mechanism for corona formation on Venus. *Icarus*, 180(2), 292–307. <https://doi.org/10.1016/j.icarus.2005.11.001>
- Houston, H. (2015). 4.13 - Deep earthquakes. In G. Schubert (Ed.), *Treatise on geophysics* (2nd ed., pp. 329–354). Elsevier. <https://doi.org/10.1016/B978-0-444-53802-4.00079-8>
- Hyndman, R. D., & Wang, K. (1993). Thermal constraints on the zone of major thrust earthquake failure: The Cascadia subduction zone. *Journal of Geophysical Research*, 98(B2), 2039–2060. <https://doi.org/10.1029/92jb02279>
- Hyndman, R. D., Yamano, M., & Oleskevich, D. A. (1997). The seismogenic zone of subduction thrust faults. *Island Arc*, 6(3), 244–260. <https://doi.org/10.1111/j.1440-1738.1997.tb00175.x>
- Ivanov, M. A., & Head, J. W. (2011). Global geological map of Venus. *Planetary and Space Science*, 59(13), 1559–1600. <https://doi.org/10.1016/j.pss.2011.07.008>
- James, P. B., Zuber, M. T., & Phillips, R. J. (2013). Crustal thickness and support of topography on Venus. *Journal of Geophysical Research: Planets*, 118(4), 859–875. <https://doi.org/10.1029/2012je004237>
- Janes, D. M., Squyres, S. W., Bindschadler, D. L., Baer, G., Schubert, G., Sharpton, V. L., & Stofan, E. R. (1992). Geophysical models for the formation and evolution of coronae on Venus. *Journal of Geophysical Research*, 97(E10), 16055–16067. <https://doi.org/10.1029/92je01689>
- Johnson, C. L., & Richards, M. A. (2003). A conceptual model for the relationship between coronae and large-scale mantle dynamics on Venus. *Journal of Geophysical Research*, 108(E6), 5058. <https://doi.org/10.1029/2002je001962>
- Jull, M. G., & Arkani-Hamed, J. (1995). The implications of basalt in the formation and evolution of mountains on Venus. *Physics of the Earth and Planetary Interiors*, 89(3–4), 163–175. [https://doi.org/10.1016/0031-9201\(95\)03015-o](https://doi.org/10.1016/0031-9201(95)03015-o)
- Jung, H., Green II, H. W., & Dobrzynetskaia, L. F. (2004). Intermediate-depth earthquake faulting by dehydration embrittlement with negative volume change. *Nature*, 428(6982), 545–549. <https://doi.org/10.1038/nature02412>
- Jurdy, D. M., & Stoddard, P. R. (2007). The coronae of Venus: Impact, plume, or other origin? In *Plates, plumes and planetary processes*. Geological Society of America. [https://doi.org/10.1130/2007.2430\(40\)](https://doi.org/10.1130/2007.2430(40))
- Karato, S.-I., & Barbot, S. (2018). Dynamics of fault motion and the origin of contrasting tectonic style between Earth and Venus. *Scientific Reports*, 8(1), 1–11. <https://doi.org/10.1038/s41598-018-30174-6>
- Kelemen, P. B., & Hirth, G. (2007). A periodic shear-heating mechanism for intermediate-depth earthquakes in the mantle. *Nature*, 446(7137), 787–790. <https://doi.org/10.1038/nature05717>
- Kiefer, W. S., & Peterson, K. (2003). Mantle and crustal structure in phoebe Regio and Devana Chasma, Venus. *Geophysical Research Letters*, 30(1), 5-1–5-4. <https://doi.org/10.1029/2002GL015762>
- Kiefer, W. S., & Swafford, L. C. (2006). Topographic analysis of Devana Chasma, Venus: Implications for rift system segmentation and propagation. *Journal of Structural Geology*, 28(12), 2144–2155. <https://doi.org/10.1016/j.jsg.2005.12.002>
- Knapmeyer, M., Oberst, J., Hauber, E., Wählisch, M., Deuchler, C., & Wagner, R. (2006). Working models for spatial distribution and level of Mars' seismicity. *Journal of Geophysical Research*, 111(E11), E11006. <https://doi.org/10.1029/2006je002708>
- Koch, D. M., & Manga, M. (1996). Neutrally buoyant diapirs: A model for Venus coronae. *Geophysical Research Letters*, 23(3), 225–228. <https://doi.org/10.1029/95gl03776>
- Kremic, T., Ghail, R., Gilmore, M., Hunter, G., Kiefer, W., Limaye, S., et al. (2020). Long-duration Venus lander for seismic and atmospheric science. *Planetary and Space Science*, 190, 104961. <https://doi.org/10.1016/j.pss.2020.104961>
- Krishnamoorthy, S., & Bowman, D. C. (2023). A “floatilla” of airborne seismometers for Venus. *Geophysical Research Letters*, 50(2), e2022GL100978. <https://doi.org/10.1029/2022gl100978>
- Krishnamoorthy, S., Komjathy, A., Cutts, J. A., Lognonne, P., Garcia, R. F., Panning, M. P., et al. (2020). *Seismology on Venus with infrasound observations from balloon and orbit* (Tech. Rep.). Sandia National Lab. (SNL-NM). <https://doi.org/10.2172/1603861>
- Ksanfomaliti, L., Zubkova, V., Morozov, N., & Petrova, E. (1982). Microseisms at the VENERA-13 and VENERA-14 landing sites. *Soviet Astronomy Letters*, 8, 241.
- Le Feuvre, M., & Wieczorek, M. A. (2011). Nonuniform cratering of the Moon and a revised crater chronology of the inner Solar System. *Icarus*, 214(1), 1–20. <https://doi.org/10.1016/j.icarus.2011.03.010>
- Lenardic, A., Jellinek, A., & Moresi, L.-N. (2008). A climate induced transition in the tectonic style of a terrestrial planet. *Earth and Planetary Science Letters*, 271(1–4), 34–42. <https://doi.org/10.1016/j.epsl.2008.03.031>
- Lognonné, P., & Johnson, C. (2015). 10.03—Planetary seismology. *Treatise on Geophysics*, 2, 65–120. <https://doi.org/10.1016/B978-0-444-53802-4.00167-6>
- Lorenz, R. D. (2012). Planetary seismology—Expectations for lander and wind noise with application to Venus. *Planetary and Space Science*, 62(1), 86–96. <https://doi.org/10.1016/j.pss.2011.12.010>
- Lourenço, D. L., Rozel, A. B., Ballmer, M. D., & Tackley, P. J. (2020). Plutonic-squishy lid: A new global tectonic regime generated by intrusive magmatism on Earth-like planets. *Geochemistry, Geophysics, Geosystems*, 21(4), e2019GC008756. <https://doi.org/10.1029/2019gc008756>
- Mackwell, S., Zimmerman, M., & Kohlstedt, D. (1998). High-temperature deformation of dry diabase with application to tectonics on Venus. *Journal of Geophysical Research*, 103(B1), 975–984. <https://doi.org/10.1029/97jb02671>
- Maia, J. S., & Wieczorek, M. A. (2022). Lithospheric structure of Venusian crustal plateaus. *Journal of Geophysical Research: Planets*, 127(2), e2021JE007004. <https://doi.org/10.1029/2021je007004>
- Maia, J. S., Wieczorek, M. A., & Plesa, A. (2023). The mantle viscosity structure of Venus. *Geophysical Research Letters*, 50(15), e2023GL103847. <https://doi.org/10.1029/2023gl103847>
- Marcq, E., Bertaux, J.-L., Montmessin, F., & Belyaev, D. (2013). Variations of sulphur dioxide at the cloud top of Venus's dynamic atmosphere. *Nature Geoscience*, 6(1), 25–28. <https://doi.org/10.1038/ngeo1650>
- McGill, G. E., Steenstrup, S. J., Barton, C., & Ford, P. G. (1981). Continental rifting and the origin of Beta Regio, Venus. *Geophysical Research Letters*, 8(7), 737–740. <https://doi.org/10.1029/g1008i007p00737>
- McKenzie, D., Jackson, J., & Priestley, K. (2005). Thermal structure of oceanic and continental lithosphere. *Earth and Planetary Science Letters*, 233(3–4), 337–349. <https://doi.org/10.1016/j.epsl.2005.02.005>
- McKinnon, W. B., Zahnle, K. J., Ivanov, B. A., & Melosh, H. (1997). Cratering on Venus: Models and observations. In *Venus II: Geology, geophysics, atmosphere, and solar wind environment* (p. 969). Retrieved from [muse.jhu.edu/book/98963](https://muse.jhu.edu/book/98963)
- Melgar, D., Ruiz-Angulo, A., Garcia, E. S., Manea, M., Manea, V. C., Xu, X., et al. (2018). Deep embrittlement and complete rupture of the lithosphere during the  $M_w$  8.2 Tehuantepec earthquake. *Nature Geoscience*, 11(12), 955–960. <https://doi.org/10.1038/s41561-018-0229-y>
- Molnar, P. (2020). The brittle-plastic transition, earthquakes, temperatures, and strain rates. *Journal of Geophysical Research: Solid Earth*, 125(7), e2019JB019335. <https://doi.org/10.1029/2019jb019335>

- Musser, G. S., Jr., & Squyres, S. W. (1997). A coupled thermal-mechanical model for corona formation on Venus. *Journal of Geophysical Research*, *102*(E3), 6581–6595. <https://doi.org/10.1029/96je03044>
- Nakamura, Y., Latham, G. V., & Dorman, H. J. (1982). Apollo lunar seismic experiment—Final summary. *Journal of Geophysical Research*, *87*(S01), A117–A123. <https://doi.org/10.1029/jb087is01p0a117>
- Namiki, N., & Solomon, S. C. (1998). Volcanic degassing of argon and helium and the history of crustal production on Venus. *Journal of Geophysical Research*, *103*(E2), 3655–3677. <https://doi.org/10.1029/97je03032>
- Nichols, D. (2022). Coloring for colorblindness. Retrieved from <http://tsitsul.in/blog/coloropt/>
- Oberst, J. (1987). Unusually high stress drops associated with shallow moonquakes. *Journal of Geophysical Research*, *92*(B2), 1397–1405. <https://doi.org/10.1029/jb092ib02p01397>
- O'Rourke, J., Wilson, C., Borrelli, M., Byrne, P. K., Dumoulin, C., Ghail, R., et al. (2023). Venus, the planet: Introduction to the evolution of Earth's sister planet. *Space Science Reviews*, *219*(1), 10. <https://doi.org/10.1007/s11214-023-00956-0>
- Pavri, B., Head, J. W., III, Klose, K. B., & Wilson, L. (1992). Steep-sided domes on Venus: Characteristics, geologic setting, and eruption conditions from Magellan data. *Journal of Geophysical Research*, *97*(E8), 13445–13478. <https://doi.org/10.1029/92je01162>
- Peacock, S. M. (2001). Are the lower planes of double seismic zones caused by serpentine dehydration in subducting oceanic mantle? *Geology*, *29*(4), 299–302. [https://doi.org/10.1130/0091-7613\(2001\)029<0299:atpod>2.0.co;2](https://doi.org/10.1130/0091-7613(2001)029<0299:atpod>2.0.co;2)
- Peacock, S. M., & Hyndman, R. D. (1999). Hydrous minerals in the mantle wedge and the maximum depth of subduction thrust earthquakes. *Geophysical Research Letters*, *26*(16), 2517–2520. <https://doi.org/10.1029/1999gl900558>
- Pettengill, G. (1992). *MGN V radar system derived MIDR compressed thrice V1.0*. NASA Planetary Data System. Retrieved from <https://pds.nasa.gov/ds-view/pds/viewProfile.jsp?dsid=MGN-V-RDRS-5-MIDR-C3-V1.0>
- Phillips, R. J., Kaula, W. M., McGill, G. E., & Malin, M. C. (1981). Tectonics and evolution of Venus. *Science*, *212*(4497), 879–887. <https://doi.org/10.1126/science.212.4497.879>
- Phillips, R. J., & Malin, M. C. (1984). Tectonics of Venus. *Annual Review of Earth and Planetary Sciences*, *12*(1), 411–443. <https://doi.org/10.1146/annurev.earth.12.1.411>
- Piskorz, D., Elkins-Tanton, L. T., & Smrekar, S. E. (2014). Coronae formation on Venus via extension and lithospheric instability. *Journal of Geophysical Research: Planets*, *119*(12), 2568–2582. <https://doi.org/10.1002/2014je004636>
- Price, M., & Suppe, J. (1995). Constraints on the resurfacing history of Venus from the hypsometry and distribution of volcanism, tectonism, and impact craters. *Earth, Moon, and Planets*, *71*(1–2), 99–145. <https://doi.org/10.1007/bf00612873>
- Price, M., Watson, G., Suppe, J., & Brankman, C. (1996). Dating volcanism and rifting on Venus using impact crater densities. *Journal of Geophysical Research*, *101*(E2), 4657–4671. <https://doi.org/10.1029/95je03017>
- Prieto, G. A., Froment, B., Yu, C., Poli, P., & Abercrombie, R. (2017). Earthquake rupture below the brittle-ductile transition in continental lithospheric mantle. *Science Advances*, *3*(3), e1602642. <https://doi.org/10.1126/sciadv.1602642>
- Regorda, A., Thieulot, C., Van Zelst, I., Erdős, Z., Maia, J., & Buitser, S. (2023). Rifting Venus: Insights from numerical modeling. *Journal of Geophysical Research: Planets*, *128*(3), e2022JE007588. <https://doi.org/10.1029/2022JE007588>
- Richards, F., Hoggard, M., Cowton, L., & White, N. (2018). Reassessing the thermal structure of oceanic lithosphere with revised global inventories of basement depths and heat flow measurements. *Journal of Geophysical Research: Solid Earth*, *123*(10), 9136–9161. <https://doi.org/10.1029/2018jb015998>
- Rolf, T., Weller, M., Gülcher, A., Byrne, P., O'Rourke, J. G., Herrick, R., et al. (2022). Dynamics and evolution of Venus' mantle through time. *Space Science Reviews*, *218*(8), 70. <https://doi.org/10.1007/s11214-022-00937-9>
- Romeo, I., & Turcotte, D. (2008). Pulsating continents on Venus: An explanation for crustal plateaus and tessera terrains. *Earth and Planetary Science Letters*, *276*(1–2), 85–97. <https://doi.org/10.1016/j.epsl.2008.09.009>
- Sabbeth, L., Carrington, M. A., & Smrekar, S. E. (2024). Constraints on corona formation from an analysis of topographic rims and fracture annuli. *Earth and Planetary Science Letters*, *633*, 118568. <https://doi.org/10.1016/j.epsl.2024.118568>
- Sabbeth, L., Smrekar, S., & Stock, J. (2023a). Estimated seismicity of Venusian wrinkle ridges based on fault scaling relationships. *Earth and Planetary Science Letters*, *619*, 118308. <https://doi.org/10.1016/j.epsl.2023.118308>
- Sabbeth, L., Smrekar, S. E., & Stock, J. M. (2023b). Using InSight data to calibrate seismicity from remote observations of surface faulting. *Journal of Geophysical Research: Planets*, *128*(6), e2022JE007686. <https://doi.org/10.1029/2022JE007686>
- Salvador, A., Avicé, G., Breuer, D., Gillmann, C., Jacobson, S., Lammer, H., et al. (2022). Magma ocean, water, and the early atmosphere of Venus. *Space Science Reviews*, *219*(7), 51. <https://doi.org/10.1007/s11214-023-00995-7>
- Scholz, C. H. (2019). *The mechanics of earthquakes and faulting*. Cambridge University Press. <https://doi.org/10.1017/9781316681473>
- Schools, J., & Smrekar, S. E. (2024). Formation of coronae topography and fractures via plume buoyancy and melting. *Earth and Planetary Science Letters*, *633*, 118643. <https://doi.org/10.1016/j.epsl.2024.118643>
- Schubert, G., & Sandwell, D. (1995). A global survey of possible subduction sites on Venus. *Icarus*, *117*(1), 173–196. <https://doi.org/10.1006/icar.1995.1150>
- Seno, T. (2009). Determination of the pore fluid pressure ratio at seismogenic megathrusts in subduction zones: Implications for strength of asperities and Andean-type mountain building. *Journal of Geophysical Research*, *114*(B5), B05405. <https://doi.org/10.1029/2008jb005889>
- Seton, M., Müller, R. D., Zahirovic, S., Williams, S., Wright, N. M., Cannon, J., et al. (2020). A global data set of present-day oceanic crustal age and seafloor spreading parameters. *Geochemistry, Geophysics, Geosystems*, *21*(10), e2020GC009214. <https://doi.org/10.1029/2020gc009214>
- Smrekar, S. E., Davaille, A., & Sotin, C. (2018). Venus interior structure and dynamics. *Space Science Reviews*, *214*(5), 1–34. <https://doi.org/10.1007/s11214-018-0518-1>
- Smrekar, S. E., Dyar, D., Helbert, J., Hensley, S., Nunes, D., & Whitten, J. (2020). VERITAS (Venus Emissivity, Radio Science, InSAR, Topography, and Spectroscopy): A proposed Discovery mission. In *European planetary science congress* (p. EPSC2020-447). <https://doi.org/10.5194/epsc2020-447>
- Smrekar, S. E., Ostberg, C., & O'Rourke, J. G. (2023). Earth-like lithospheric thickness and heat flow on Venus consistent with active rifting. *Nature Geoscience*, *16*(1), 13–18. <https://doi.org/10.1038/s41561-022-01068-0>
- Smrekar, S. E., & Sotin, C. (2012). Constraints on mantle plumes on Venus: Implications for volatile history. *Icarus*, *217*(2), 510–523. <https://doi.org/10.1016/j.icarus.2011.09.011>
- Smrekar, S. E., & Stofan, E. R. (1997). Corona formation and heat loss on Venus by coupled upwelling and delamination. *Science*, *277*(5330), 1289–1294. <https://doi.org/10.1126/science.277.5330.1289>
- Smrekar, S. E., & Stofan, E. R. (1999). Origin of corona-dominated topographic rises on Venus. *Icarus*, *139*(1), 100–115. <https://doi.org/10.1006/icar.1999.6090>
- Smrekar, S. E., Stofan, E. R., Mueller, N., Treiman, A., Elkins-Tanton, L., Helbert, J., et al. (2010). Recent hotspot volcanism on Venus from VIRTIS emissivity data. *Science*, *328*(5978), 605–608. <https://doi.org/10.1126/science.1186785>

- Solomon, S. C. (1993). The geophysics of Venus. *Physics Today*, 46(7), 48–55. <https://doi.org/10.1063/1.881359>
- Solomon, S. C., Bullock, M. A., & Grinspoon, D. H. (1999). Climate change as a regulator of tectonics on Venus. *Science*, 286(5437), 87–90. <https://doi.org/10.1126/science.286.5437.87>
- Solomon, S. C., Head, J. W., Kaula, W. M., McKenzie, D., Parsons, B., Phillips, R. J., et al. (1991). Venus tectonics: Initial analysis from Magellan. *Science*, 252(5003), 297–312. <https://doi.org/10.1126/science.252.5003.297>
- Spencer, J. E. (2001). Possible giant metamorphic core complex at the center of Artemis corona, Venus. *Geological Society of America Bulletin*, 113(3), 333–345. [https://doi.org/10.1130/0016-7606\(2001\)113<0333:pgmcca>2.0.co;2](https://doi.org/10.1130/0016-7606(2001)113<0333:pgmcca>2.0.co;2)
- Squyres, S. W., Janes, D., Baer, G., Bindschadler, D. L., Schubert, G., Sharpton, V. L., & Stofan, E. R. (1992). The morphology and evolution of coronae on Venus. *Journal of Geophysical Research*, 97(E8), 13611–13634. <https://doi.org/10.1029/92je01213>
- Stein, S., & Wysession, M. (2009). *An introduction to seismology, earthquakes, and Earth structure*. John Wiley & Sons.
- Stevenson, D. J., Cutts, J. A., Mimoun, D., Arrowsmith, S., Banerdt, W. B., Blom, P., et al. (2015). *Probing the interior structure of Venus*. Keck Institute for Space Studies. <https://doi.org/10.26206/C1CX-EV12>
- Stoddard, P. R., & Jurdy, D. M. (2012). Topographic comparisons of uplift features on Venus and Earth: Implications for Venus tectonics. *Icarus*, 217(2), 524–533. <https://doi.org/10.1016/j.icarus.2011.09.003>
- Stofan, E. R., Saunders, R., Senske, D., Nock, K., Tralli, D., Lundgren, P., et al. (1993). Venus interior structure mission (VISM): Establishing a seismic network on Venus. In *Advanced technologies for planetary instruments*.
- Stofan, E. R., Bindschadler, D. L., Head, J. W., & Parmentier, E. M. (1991). Corona structures on Venus: Models of origin. *Journal of Geophysical Research*, 96(E4), 20933–20946. <https://doi.org/10.1029/91je02218>
- Stofan, E. R., Sharpton, V. L., Schubert, G., Baer, G., Bindschadler, D. L., Janes, D. M., & Squyres, S. W. (1992). Global distribution and characteristics of coronae and related features on Venus: Implications for origin and relation to mantle processes. *Journal of Geophysical Research*, 97(E8), 13347–13378. <https://doi.org/10.1029/92je01314>
- Stofan, E. R., Smrekar, S. E., Bindschadler, D. L., & Senske, D. A. (1995). Large topographic rises on Venus: Implications for mantle upwelling. *Journal of Geophysical Research*, 100(E11), 23317–23328. <https://doi.org/10.1029/95JE01834>
- Strom, R. G., Schaber, G. G., & Dawson, D. D. (1994). The global resurfacing of Venus. *Journal of Geophysical Research*, 99(E5), 10899–10926. <https://doi.org/10.1029/94je00388>
- Sulcanese, D., Mitri, G., & Mastrogioseppe, M. (2024). Evidence of ongoing volcanic activity on Venus revealed by Magellan radar. *Nature Astronomy*, 1–10. <https://doi.org/10.1038/s41550-024-02272-1>
- Tian, Y., Herrick, R. R., West, M. E., & Kremic, T. (2023). Mitigating power and memory constraints on a Venusian seismometer. *Seismological Society of America*, 94(1), 159–171. <https://doi.org/10.1785/0220220085>
- Tichelaar, B. W., & Ruff, L. J. (1993). Depth of seismic coupling along subduction zones. *Journal of Geophysical Research*, 98(B2), 2017–2037. <https://doi.org/10.1029/92jb02045>
- van Dinther, Y., Gerya, T. V., Dalguer, L. A., Corbi, F., Funicello, F., & Mai, P. M. (2013). The seismic cycle at subduction thrusts: 2. Dynamic implications of geodynamic simulations validated with laboratory models. *Journal of Geophysical Research: Solid Earth*, 118(4), 1502–1525. <https://doi.org/10.1029/2012jb009479>
- van Dinther, Y., Gerya, T. V., Dalguer, L. A., Mai, P. M., Morra, G., & Giardini, D. (2013). The seismic cycle at subduction thrusts: Insights from seismo-thermo-mechanical models. *Journal of Geophysical Research: Solid Earth*, 118(12), 6183–6202. <https://doi.org/10.1002/2013jb010380>
- van Dinther, Y., Mai, P. M., Dalguer, L. A., & Gerya, T. V. (2014). Modeling the seismic cycle in subduction zones: The role and spatiotemporal occurrence of off-megathrust earthquakes. *Geophysical Research Letters*, 41(4), 1194–1201. <https://doi.org/10.1002/2013gl058886>
- Van Zelst, I. (2022). Comment on “Estimates on the frequency of volcanic eruptions on Venus” by Byrne & Krishnamoorthy (2022). *Journal of Geophysical Research: Planets*, 127(12), e2022JE007448. <https://doi.org/10.1029/2022JE007448>
- Van Zelst, I., Maia, J., Plesa, A.-C., Ghail, R., & Spühler, M. (2024). Data & scripts - Estimates on the possible annual seismicity of Venus [Dataset]. *Zenodo*. <https://doi.org/10.5281/zenodo.10539250>
- Van Zelst, I., Thieulot, C., & Craig, T. J. (2023). The effect of temperature-dependent material properties on simple thermal models of subduction zones. *Solid Earth*, 14(7), 683–707. <https://doi.org/10.5194/se-14-683-2023>
- Van Zelst, I., Wollherr, S., Gabriel, A.-A., Madden, E. H., & van Dinther, Y. (2019). Modeling megathrust earthquakes across scales: One-way coupling from geodynamics and seismic cycles to dynamic rupture. *Journal of Geophysical Research: Solid Earth*, 124(11), 11414–11446. <https://doi.org/10.1029/2019JB017539>
- Wang, J., Zhao, D., & Yao, Z. (2017). Seismic anisotropy evidence for dehydration embrittlement triggering intermediate-depth earthquakes. *Scientific Reports*, 7(1), 1–9. <https://doi.org/10.1038/s41598-017-02563-w>
- Weller, M., Lenardic, A., & O'Neill, C. (2015). The effects of internal heating and large scale climate variations on tectonic bi-stability in terrestrial planets. *Earth and Planetary Science Letters*, 420, 85–94. <https://doi.org/10.1016/j.epsl.2015.03.021>
- Widemann, T., Smrekar, S. E., Garvin, J. B., Straume-Lindner, A. G., Ocampo, A. C., Schulte, M. D., et al. (2023). Venus evolution through time: Key science questions, selected mission concepts and future investigations. *Space Science Reviews*, 219(7), 56. <https://doi.org/10.1007/s11214-023-00992-w>
- Wieczorek, M. A. (2015). Spherical harmonic model of the planet Venus: VenusTopo719 [Dataset]. *Zenodo*. <https://doi.org/10.5281/zenodo.3870925>
- Williams, N. R., Bell, J. F., III., Watters, T. R., Banks, M. E., Daud, K., & French, R. A. (2019). Evidence for recent and ancient faulting at Mare Frigoris and implications for lunar tectonic evolution. *Icarus*, 326, 151–161. <https://doi.org/10.1016/j.icarus.2019.03.002>
- Wright, T. J., Elliott, J. R., Wang, H., & Ryder, I. (2013). Earthquake cycle deformation and the Moho: Implications for the rheology of continental lithosphere. *Tectonophysics*, 609, 504–523. <https://doi.org/10.1016/j.tecto.2013.07.029>
- Yamasaki, T., & Seno, T. (2003). Double seismic zone and dehydration embrittlement of the subducting slab. *Journal of Geophysical Research*, 108(B4), 2212. <https://doi.org/10.1029/2002jb001918>
- Zhong, S.-S., Zhao, Y.-Y. S., Lin, H., Chang, R., Qi, C., Wang, J., et al. (2023). High-temperature oxidation of magnesium- and iron-rich olivine under a CO<sub>2</sub> atmosphere: Implications for Venus. *Remote Sensing*, 15(8), 1959. <https://doi.org/10.3390/rs15081959>
- Zuber, M. (1990). Ridge belts: Evidence for regional- and local-scale deformation on the surface of Venus. *Geophysical Research Letters*, 17(9), 1369–1372. <https://doi.org/10.1029/g1017i009p01369>